frontiers in Marine Science

ORIGINAL RESEARCH
published: 20 August 2019
doi: 10.3389/fmars.2019.00495

Recent Eruptions Between 2012 and 2018 Discovered at West Mata Submarine Volcano (NE Lau Basin, SW Pacific) and Characterized by New Ship, AUV, and ROV Data

William W. Chadwick Jr.[1], Kenneth H. Rubin[2], Susan G. Merle[3], Andra M. Bobbitt[3], Tom Kwasnitschka[4] and Robert W. Embley[3]*

[1] NOAA Pacific Marine Environmental Laboratory, Newport, OR, United States, [2] Department of Earth Sciences, University of Hawai'i at Mānoa, Honolulu, HI, United States, [3] CIMRS, Oregon State University, Newport, OR, United States, [4] GEOMAR, Helmholtz Centre for Ocean Research, Kiel, Germany

West Mata is a submarine volcano located in the SW Pacific Ocean between Fiji and Samoa in the NE Lau Basin. West Mata was discovered to be actively erupting at its summit in September 2008 and May 2009. Water-column chemistry and hydrophone data suggest it was probably continuously active until early 2011. Subsequent repeated bathymetric surveys of West Mata have shown that it changed to a style of frequent but intermittent eruptions away from the summit since then. We present new data from ship-based bathymetric surveys, high-resolution bathymetry from an autonomous underwater vehicle, and observations from remotely operated vehicle dives that document four additional eruptions between 2012 and 2018. Three of those eruptions occurred between September 2012 and March 2016; one near the summit on the upper ENE rift, a second on the NE flank away from any rift zone, and a third at the NE base of the volcano. The latter intruded a sill into a basin with thick sediments, uplifted them, and then extruded lava onto the seafloor around them. The most recent of the four eruptions occurred between March 2016 and November 2017 along the middle ENE rift zone and produced pillow lava flows with a shingled morphology and tephra as well as clastic debris that mantled the SE slope. ROV dive observations show that the shallower recent eruptions at West Mata include a substantial pyroclastic component, based on thick (>1 m) tephra deposits near eruptive vents. The deepest eruption sites lack these near-vent tephra deposits, suggesting that pyroclastic activity is minimal below ~2500 mbsl. The multibeam sonar re-surveys constrain the timing, thickness, area, morphology, and volume of the new eruptions. The cumulative erupted volume since 1996 suggests that eruptions at West Mata are volume-predictable with an average eruption rate of 7.8×10^6 m^3/yr. This relatively low magma supply rate and the high frequency of eruptions (every 1–2 years) suggests that the magma reservoir at West Mata is relatively small. With its frequent activity, West Mata continues to be an ideal natural laboratory for the study of submarine volcanic eruptions.

Keywords: submarine volcanoes, submarine eruptions, seafloor mapping, bathymetry changes, multibeam sonar surveying, lava flow morphology, pyroclastic activity, autonomous and remotely operated underwater vehicle

OPEN ACCESS

Edited by:
Cristina Gambi,
Marche Polytechnic University, Italy

Reviewed by:
Paraskevi Nomikou,
National and Kapodistrian University of Athens, Greece
Simon James Barker,
Victoria University of Wellington, New Zealand

****Correspondence:***
William W. Chadwick Jr.
william.w.chadwick@noaa.gov

Specialty section:
This article was submitted to Deep-Sea Environments and Ecology, a section of the journal Frontiers in Marine Science

Received: *02 April 2019*
Accepted: *22 July 2019*
Published: *20 August 2019*

Citation:
Chadwick WW Jr, Rubin KH, Merle SG, Bobbitt AM, Kwasnitschka T and Embley RW (2019) Recent Eruptions Between 2012 and 2018 Discovered at West Mata Submarine Volcano (NE Lau Basin, SW Pacific) and Characterized by New Ship, AUV, and ROV Data. Front. Mar. Sci. 6:495. doi: 10.3389/fmars.2019.00495

INTRODUCTION

We learn the most about active volcanic processes by directly observing them, a fact that motivates the establishment of observatories at Earth's most active volcanoes. Eruptions that occur on land have obvious manifestations, making them easy targets for enhanced observation and study, but detecting and observing volcanic eruptions in the deep sea is much more difficult (Rubin et al., 2012), despite the fact that most of Earth's volcanic output occurs in the oceans (Crisp, 1984). Frequently active submarine volcanoes provide a rare and valuable opportunity to learn about the underwater processes associated with individual eruptions as well as how a submarine volcano's activity evolves with time (Staudigel et al., 2006; Watts et al., 2012; Schnur et al., 2017; Allen et al., 2018; Wilcock et al., 2018). West Mata is of special interest because it is an excellent example of such a site.

West Mata is a frequently active submarine volcano with a summit depth at ∼1200 meters below sea level (mbsl) and a base at nearly 3000 mbsl, located in the extensional NE Lau Basin between Fiji and Samoa in the SW Pacific Ocean (**Figure 1**). It is one of only two places on Earth where active submarine eruptions have been directly observed in the deep sea (>500 mbsl depth) (Resing et al., 2011; Rubin et al., 2012). It is also by far the deepest since the other site is NW Rota-1 Seamount in the Mariana arc, which has a summit depth of 517 mbsl (Embley et al., 2006; Chadwick et al., 2008, 2012; Deardorff et al., 2011; Schnur et al., 2017). West Mata is also unique because it is the only known site where lava of boninite composition is being erupted in a modern tectonic setting, a composition often associated with nascent inter-oceanic subduction (Resing et al., 2011; Rubin et al., 2018). West Mata is the largest of nine volcanoes with similar morphology and composition, comprising the "Mata Group," all elongate cones with roughly parallel rift zones that are oriented in a WSW-ENE direction (**Figure 1**), suggesting a regional structural control (Clague et al., 2011; Rubin et al., 2018).

The Mata Group volcanoes lie in a "rear-arc" tectonic setting, between the Tonga volcanic arc to the east, and the NE Lau back-arc spreading center to the west, and in-board of the nearly 90° bend at the northern terminus of the Tonga trench, where it transitions into a plate boundary transform zone (**Figure 1**). The NE Lau Basin hosts the world's highest subduction rates (Bevis et al., 1995) and the fastest opening back-arc basin (Zellmer and Taylor, 2001), which creates an extraordinary concentration and diversity of submarine volcanism in the area (Embley and Rubin, 2018; Rubin et al., 2018) and also hosts an extraordinary number of active hydrothermal vent sites (Baker et al., 2019).

This paper presents new results from West Mata including depth changes between repeated bathymetric surveys from ships, high-resolution mapping from autonomous underwater vehicles (AUVs), and visual observations of the seafloor from remotely operated vehicles (ROVs). The new data reveal and characterize six eruptions at West Mata (**Figure 2**), a collapse pit at the summit, and a landslide scar just east of the summit that all occurred after eruptive activity was first observed at the summit in May 2009 (Resing et al., 2011; Embley et al., 2014). These new observations show that the eruptive style at West Mata changed from continuous to episodic during this time period. The observations also provide information about the character of individual eruptions at different depths, because they span the entire volcano from the summit to abyssal depths (**Figure 2**). We show that the recent eruptions define a linear trend in erupted volume with time, which has implications for the magma supply, the volume of magma storage within the volcano, and the future behavior of the volcano.

PREVIOUS WORK

West Mata first gained attention in November 2008 during a regional hydrographic survey that discovered an intense hydrothermal plume over the summit with high levels of hydrogen and shards of volcanic glass, suggesting it was actively erupting at the time (Resing et al., 2011; Baumberger et al., 2014). This led to a rapid-response expedition 6 months later in May 2009 with ROV *Jason* (Resing et al., 2011) that found two active eruptive vents on the north side of the summit ridge, named Hades and Prometheus. The eruptive activity was continuous at moderate to low effusion rates, and was characterized by explosive bursts that produced both pillow lavas and pyroclasts, especially when large bubbles of magmatic gases up to ∼1 m in diameter (presumably SO_2, CO_2, H_2O) were expelled from the vent (Resing et al., 2011).

During that same expedition in May 2009, the summit and rift zones were mapped at high-resolution (1 m) with the MBARI AUV *D. Allan B.* (Clague et al., 2011; Clague, 2015), revealing the setting of the Hades and Prometheus eruptive vents within embayments of the summit ridge on the upper north slope of the volcano. The high-resolution AUV bathymetry also highlighted the contrast in morphology between the smooth north and south slopes of the volcano, which are covered with volcaniclastic debris shed from vents near the summit, and the hummocky lava flows evident on the ENE and WSW rift zones. The rift zone flows have a distinctive morphology with flat tops and steep sides and are typically arranged in a shingled arrangement along the sloping rift zone axis, locally modified by landslides. Clague et al. (2011) also compared the first ship-based bathymetric survey at West Mata in 1996 to later ones collected in 2008–2010 and found large depth changes at the summit (up to 88 m shallower) and on north flank (up to 96 m shallower), suggesting that eruptive activity from the summit vents had been dominant for more than a decade and had produced thick volcaniclastic deposits on the north flank.

Additional evidence that the eruptive activity directly observed during the brief ROV dives in May 2009 was continuous and prolonged for months to years comes from local and regional hydrophone studies, radiometric dating, and repeated hydrothermal plume measurements in the water column over the volcano. A moored hydrophone deployed ∼48 km SW of West Mata recorded the sounds of continuous but variable eruptive activity at West Mata from January to May 2009 (Resing et al., 2011). During the May 2009 ROV dives, a portable hydrophone characterized from close range the eruptive activity at Hades and Prometheus, which was continuous during the several days of recordings (Dziak et al., 2015). A regional hydrophone array in the Lau Basin ∼650 km to the SSW recorded sustained

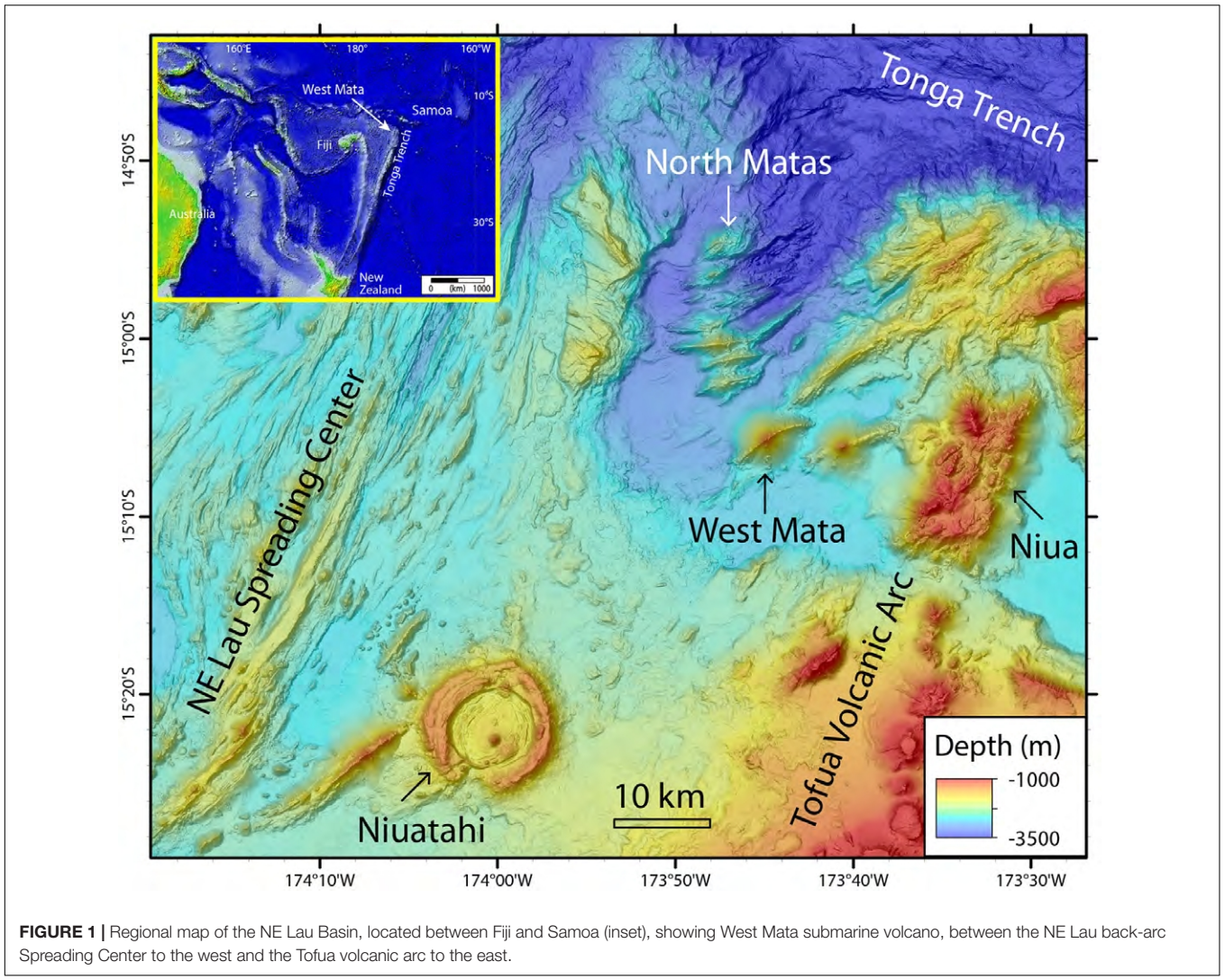

FIGURE 1 | Regional map of the NE Lau Basin, located between Fiji and Samoa (inset), showing West Mata submarine volcano, between the NE Lau back-arc Spreading Center to the west and the Tofua volcanic arc to the east.

low-level activity in the direction of West Mata between January 2009 and April 2010 (Bohnenstiehl et al., 2014). Another local hydrophone array was moored 5–15 km away from the summit from December 2009 to August 2011 and recorded continuous eruptive activity until late 2010, when it began to decline and eventually stopped by February 2011 (Embley et al., 2014; Dziak et al., 2015). Radiometric dating of lavas collected at or near the summit in 2009 and 2012 using short-lived ^{210}Po-^{210}Pb disequilibrium confirmed that effusive volcanism spanned at least April 2007 to December 2010 (Embley et al., 2014).

During the period of continuous eruptive activity, turbidity sensors on one of the hydrophone moorings and on conductivity, temperature, depth (CTD) instruments during infrequent ship-based vertical hydrographic casts showed evidence for occasional mass-wasting events down the flanks of West Mata (Dziak et al., 2015; Walker et al., under review[1]). Similarly, submarine landslides were detected on the north flank of West Mata by the local moored hydrophones between December 2009 and May 2010 (Caplan-Auerbach et al., 2014). Ship-based CTD casts over the summit in November 2008, May 2009, April/May 2010, and September 2012 showed a gradual decrease in the strength of chemical and particle signals in the hydrothermal plume above the summit of West Mata during this time period, consistent with the hydrophone data (Baumberger et al., 2014).

ROV dives in September 2012 confirmed that West Mata was no longer erupting continuously from the summit vents (Embley et al., 2014). Instead, a pit crater ∼200 m wide and ∼100 m deep had formed at the former location of Hades vent. Later analysis of additional repeated ship-based bathymetric surveys from 1996 to 2012 (**Figure 2**) revealed the first evidence for episodic eruptive activity on the rift zones (Embley et al., 2014). Here, we build on those results with the first direct observations of recent eruption sites away from the summit at West Mata from AUV and ROV dives, as well as new evidence for four additional episodic eruption sites on and near the rift zones between 2012 and 2018.

[1]Walker, S. L., Baker, E. T., Lupton, J. E., and Resing, J. A. (under review). Patterns of fine ash dispersal related to volcanic activity at West Mata volcano, NE Lau Basin. *Front. Mar. Sci.*

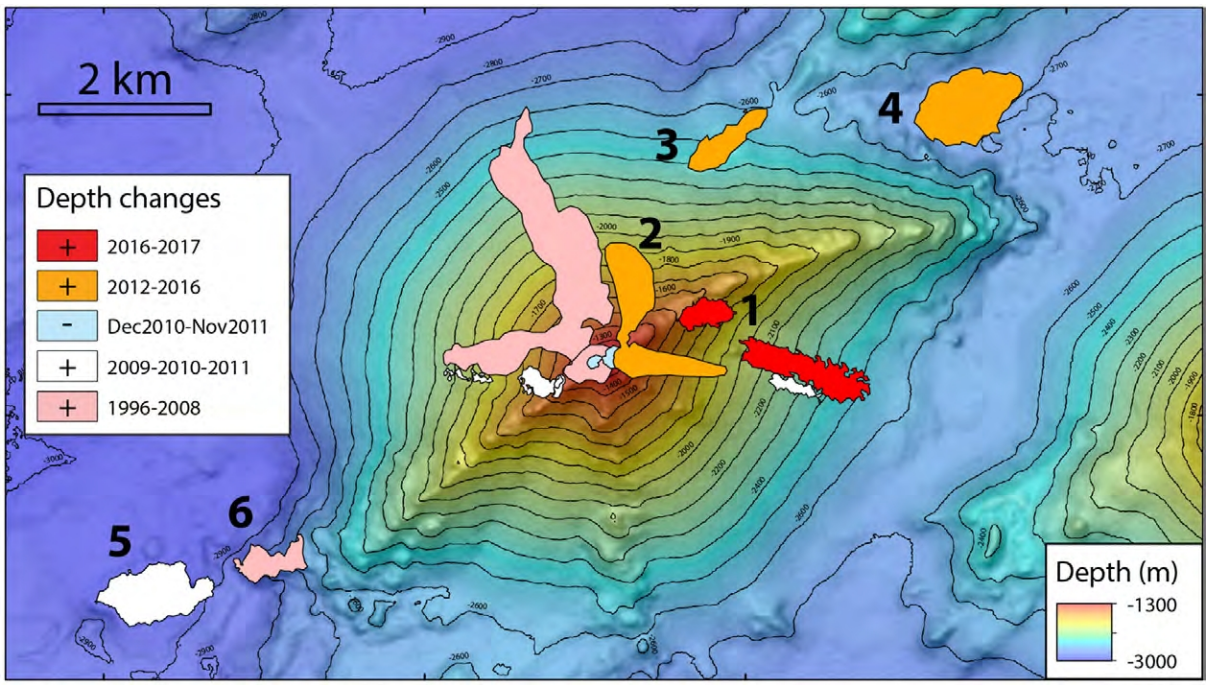

FIGURE 2 | Map of West Mata showing areas where depth changes have been found by repeated bathymetric surveys between 1996 and 2018, documenting recent eruption sites. Those from 1996 to 2012 are from Clague et al. (2011) and Embley et al. (2014); those after 2012 are new (orange and red areas, see legend). The depth changes shown in white are several grouped together within a longer time window (2009–2012) than the time constraints on individual sites (see Embley et al., 2014). The blue areas are negative depth changes from a summit collapse and landslide. Numbers indicate eruption sites discussed in detail in this paper.

MATERIALS AND METHODS

The main method we use for documenting recent eruptions at West Mata is identifying significant depth changes between repeated ship-based multibeam sonar bathymetric surveys. The volcano has been mapped nine times between 1996 and 2018, with eight of those since 2008 (**Table 1** and **Figure 3**). The first survey in 1996 was collected with a lower resolution sonar system and before reliable GPS navigation, so it is notably lower in quality and comparisons with it have higher uncertainty [as discussed by Clague et al. (2011) and Embley et al. (2014)]. Nevertheless, all the surveys since 2008 are of relatively high quality and we generally can use a threshold to identify significant depth changes of ±10 m. Still, not all depth changes above this threshold are real, but false positives can be eliminated by comparing with visual ground truth from submersibles and/or whether they make geologic sense, based on their location and morphology. The timing of the eruptions associated with each confirmed area of depth change is constrained by the dates of the before-and-after bathymetric surveys. All the bathymetric data at West Mata were processed using MB-System software (Caress and Chayes, 2016) and were gridded at a 25-m grid-cell spacing for this analysis.

In this paper, we focus on the depth changes discovered since those documented by Embley et al. (2014) by using the two most recent ship-based bathymetric surveys in March 2016 and in November 2017 (**Table 1**). We use the positive depth changes between bathymetric surveys to calculate the thicknesses, areas, and volumes of erupted material at each site (**Table 2**). We have not re-calculated the volumes reported by Embley et al. (2014) for the depth changes before 2012. For those after 2012, we calculate the areas and volumes of change using ArcMap GIS software by subtracting one bathymetric grid from another within a polygon that was manually drawn to isolate the area of significant depth change. We do not use the AUV bathymetry for the volume calculations because the AUV surveys do not cover all the eruption sites and so the ship data provide a more uniform and consistent way of comparing multiple events.

Most of the new data presented in this paper were collected during a two-leg expedition on *R/V Falkor* to the NE Lau Basin between 10 November and 18 December 2017 (FK171110). The first leg included dives with AUV *Sentry* to collect high-resolution (1 m) bathymetry (at 70 m altitude) and near-bottom photo surveys (at 5 m altitude) of selected areas. Four of six AUV *Sentry* dives were made at West Mata (dives 457, 458, 460, and 463) and the first three collected useful data with its Reson 7125 (200 kHz) multibeam sonar (Merle et al., 2018a); unfortunately the multibeam sonar malfunctioned during the later dive. Where they overlap, the 2017 AUV *Sentry* bathymetry can be compared with the 2009 survey by the MBARI AUV *D. Allan B.* (Clague et al., 2011; Clague, 2015).

TABLE 1 | Multibeam sonar bathymetric surveys at West Mata volcano.

Month-Year	Vessel/vehicle	Cruise ID	Chief Scientist(s)	Sonar system
June-1996	*R/V Melville*	BMRG08MV	S. Bloomer/D. Wright	Seabeam2000
November-2008	*R/V Thompson*	TN227	J. Lupton	EM300
May-2009	*R/V Thompson*	TN234	J. Resing/R. Embley	EM300
May-2009	*AUV D. Allan B.*	TN234	D. Clague/D. Caress	Reson 7125
May-2010	*R/V Kilo Moana*	KM1008	J. Resing	EM122
December-2010	*R/V Kilo Moana*	KM1024	K. Rubin/R. Embley	EM122
November-2011	*R/V Kilo Moana*	KM1129a	F. Martinez	EM122
September-2012	*R/V Revelle*	RR1211	J. Resing/R. Embley	EM122
March-2016	*R/V Falkor*	FK160320	T. Kwasnitschka	EM302
November-2017	*R/V Falkor*	FK171110	K. Rubin/W. Chadwick	EM302
November-2017	*AUV Sentry*	FK171110	K. Rubin/W. Chadwick	Reson 7125

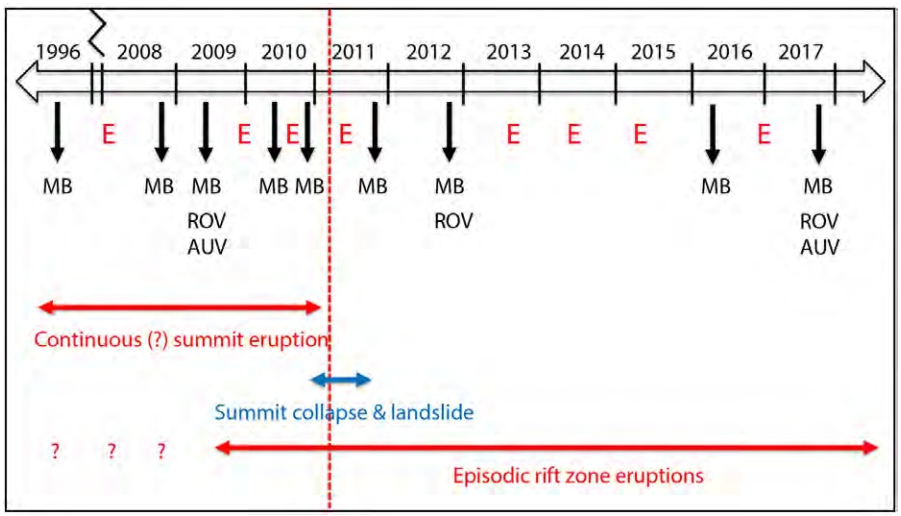

FIGURE 3 | The timeline showing the timing of multibeam sonar bathymetric surveys (MB), AUV and ROV dives in 2009, 2012, and 2017, and the transition in eruptive style from continuous summit activity to episodic rift zone eruptions (represented by red "E's" below the timeline).

TABLE 2 | Estimates of the thicknesses, areas, and volumes of recent eruption sites at West Mata based on depth changes between ship-based bathymetric surveys.

Site name	Bathymetric survey comparison (mo/years)	Geographic area and depth	Mean depth change in meters	Maximum depth change in meters	Area of depth change (x 10^6 m^2)	Volume of depth change (x 10^6 m^3)
Eruption sites newly identified by this study						
Site 1	March 2016 – November 2017	ENE Rift @ 1500 m	26.6	71	0.6	14
Site 2	November 2011 – March 2016	ENE Rift @ 1300 m	38.6	93	0.530	13.8
Site 3	November 2011 – March 2016	NE flank @ 2400 m	27.2	57	0.250	6.7
Site 4	November 2011 – March 2016	NE Base @ 2700 m	29.2	64	0.730	17.1
Areas previously identified by Embley et al. (2014)						
Site 5	May 2010 – November 2011	WSW Rift @ 2900 m	26.2	63	0.61	16
Site 6	May 1996 – November 2008	WSW Rift @ 2700 m	53.5	101	0.22	12

During the second leg of the *R/V Falkor* expedition, dives were made with ROV *SuBastian*, and 7 of 21 dives were made at West Mata (S85–S88, S93, S95, and S103) to make visual observations and collect samples at most of the recent eruption sites documented by bathymetric depth changes. Both cruise legs collected ship-based multibeam bathymetry at West Mata and the surrounding area with the ship's EM302 sonar system (Merle et al., 2018b). Other results from this expedition are described in Rubin et al. (2018), Walker et al., under review[2], and Baker et al. (2019).

[2]Walker, S. L., Baker, E. T., Lupton, J. E., and Resing, J. A. (under review). Patterns of fine ash dispersal related to volcanic activity at West Mata volcano, NE Lau Basin. *Front. Mar. Sci.*

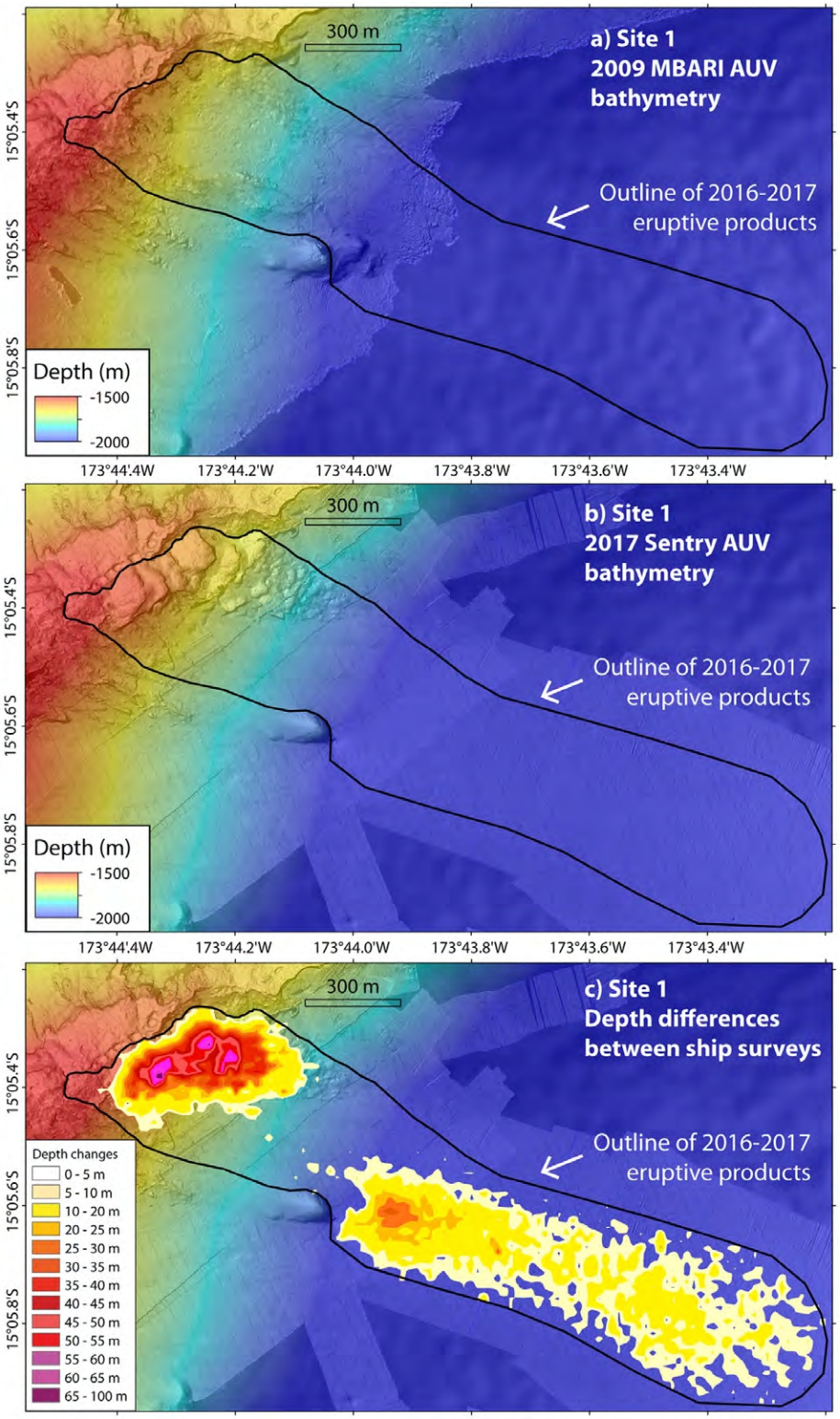

FIGURE 4 | Broad-view maps of eruption site #1, on the middle ENE rift zone of West Mata (see **Figure 2**) showing **(a)** pre-eruption MBARI AUV bathymetry from 2009, **(b)** post-eruption *Sentry* AUV bathymetry from 2017, and **(c)** positive depth differences between ship-based surveys in 2016 and 2017 overlain on 2017 AUV bathymetry (see **Table 2**). Black outlines enclose the site #1 eruption deposits. In this and subsequent figures, the pre-eruption AUV bathymetry was collected in May 2009 by the MBARI AUV *D. Allan B.* (Clague et al., 2011; Clague, 2015), and the post-eruption AUV bathymetry is from surveys in November 2017 with AUV *Sentry* (Merle et al., 2018a).

RESULTS

The summary timeline in **Figure 3** shows the timing of all the ship-based multibeam sonar bathymetric surveys at West Mata between 1996–2018 (black arrows labeled with "MB"), as well as the years with ROV and AUV dives, and how the new data reported here fit into the longer time-series of observations. Remarkably, there is evidence for eruptive activity between almost every bathymetric survey, except between the surveys less than a year apart in 2008 and 2009, and those in 2011 and 2012, which showed no change. The red "E's" in **Figure 3** denote episodic eruptions on the rift zones, whose timing is constrained by the bathymetric surveys. The arrows at the bottom highlight the major transition that occurred in early 2011 when the continuous eruptive activity at the summit ended (Embley et al., 2014). At about the same time, the summit collapsed and a landslide occurred on the SE flank with a headwall just east of the summit (blue arrows in **Figure 3**). Since 2011, all the eruptions at West Mata have been episodic eruptions on the rift zones. Although this was clearly a major change in eruptive behavior, note also that there was some overlap in time between the continuous and episodic activity. The first episodic rift eruption was documented between May 2009 and May 2010 (Embley et al., 2014), and there was an even earlier one sometime between the 1996 and 2008 surveys (although it's possible that event occurred before the continuous activity began).

In this section, we focus on six recent eruption sites: the four discovered on and near the ENE rift zone from the two most recent bathymetric surveys in 2016 and 2017 (sites #1–4 in **Figure 2**), and two previously identified on and near the WSW rift zone by Embley et al. (2014) where we have new data to ground-truth previous interpretations (#5–6 in **Figure 2**). We describe the eruption sites roughly from youngest to oldest, starting with the 2016–2017 site, then the three 2012–2016 eruption sites, and then the older two sites on the WSW rift. However, for the 2012–2016 sites, note that their relative ages are unknown (the positioning of the "E's" in **Figure 3** between 2012 and 2016 is arbitrary), and we therefore proceed from shallowest to deepest among those three sites. Note also that to compute depth differences at the 2012–2016 eruption sites (**Table 2**), we have chosen to compare the 2016 survey to the 2011 survey rather than the one in 2012 because the latter is noisier. So even though we show depth changes between the 2011 and 2016 surveys in the figures and tables, we know that the timing of those depth changes is constrained in time between 2012 and 2016.

Site 1: The 2016–2017 Eruption on the Middle ENE Rift at 1500 mbsl

The most recent known eruption at West Mata occurred between March 2016 and November 2017 and was discovered during the FK171110 expedition on *R/V Falkor*. This eruption was located on the middle part of the ENE rift zone, between 1.0 and 1.5 km east of, and about 300 m below the summit (**Figure 2**). **Figure 4** shows the before-and-after AUV bathymetry at the eruption site. Comparing the AUV bathymetry from 2009 and 2017 shows that the eruptive vents were located along the southern edge of the rift zone, within the headwall of a previous landslide on the SE side of the rift (**Figure 4**). The depth changes between ship-based bathymetric surveys in 2016 and 2017 were greatest near the eruptive vents where lava flows accumulated (up to 71 m thick). Smaller positive depth changes (up to 34 m) extend at least 2.2 km downslope, where the smooth texture in the post-eruption AUV bathymetry and photographs from AUV *Sentry* show that these are volcaniclastic deposits. The area between the thick lava flows and the thinner fragmental deposits downslope had small negative depth changes (up to 5–10 m, not shown in **Figure 4c**), suggesting that some scouring occurred as the volcaniclastic material moved downslope. The total area enclosing the eruptive deposits (black outline in **Figure 4**) is 0.60×10^6 m^2, and their total volume is 14.0×10^6 m^3 (**Table 2**).

A zoomed-in view of the upper part of the eruption site (**Figure 5**) shows that the new lava flows form a series of flat-topped or slightly domed plateaus with steep margins, arranged in an overlapping, shingle-like or stepped pattern, descending to the ENE in the direction parallel to the rift axis. Adjacent to the rift, there are five somewhat equi-dimensional overlapping lava plateaus, each 100–150 m across with downward steps of 20–30 m between them (**Figure 5b**). Below these are a series of lava benches that become progressively smaller and less well-defined with distance downslope, eventually merging into a hummocky lobe of pillow lava that extends 600 m from the rift (**Figure 5b**). The steep downslope margins of the lava benches and plateaus are constructional in some places, but are cut by landslide scarps in others (for example along the scalloped southern edge of the upper-most lava plateaus in **Figure 5b**). Because the lava plateaus are relatively flat-topped but were built outward from the rift on a steeply descending slope, each lava plateau is actually wedge-shaped in cross-section; the bathymetric depth-changes between the AUV surveys show that the lava plateaus are thinnest on their upslope edges and thickest on their downslope edges (**Figure 5c**). This is consistent with their mechanism of formation being similar to that of perched lava ponds on land, as proposed by Clague et al. (2011), in which the relatively flat upper surface of a flow lobe is maintained behind a levee that is constructed from overflows at the edge of the impounded lava flow. In this interpretation, the levee grows upward along with the upper surface of the ponded lava flow. In any case, this "shingled lava plateau" morphology is very common along both rift zones of West Mata.

Visual observations of the 2016–2017 eruptive deposits were made during ROV *SuBastian* dives S86 and S103 in December 2017 (**Figure 5d**). The hummocky lobe of pillow lavas on the lower reaches of the eruption site lies on a moderate slope and has a thin dusting of tephra (**Figure 6a**). Further upslope, the steep margins of the lava plateaus and lava benches are constructional in some places, formed by near-vertical intact pillow tubes (**Figure 6b**), and in other places are vertical cliffs of truncated pillows (**Figure 6c**), where they have been cut by landslides. Below the landslide headwalls are ramps of talus made up of pillow fragments (**Figure 6d**). In contrast, the upper surfaces of the lava plateaus (near the eruptive vents) consist of pillow lavas that are deeply buried by coarse volcanic tephra (**Figure 6e**). The thickness of the tephra appears to be 1–2 m,

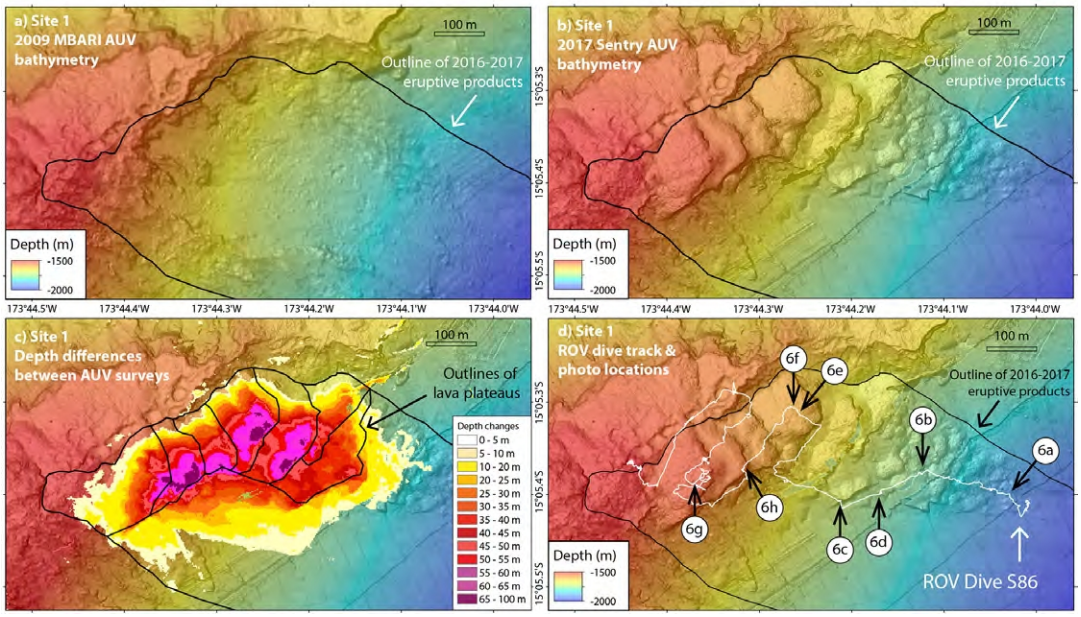

FIGURE 5 | Close-up maps of eruption site #1 showing **(a)** pre-eruption MBARI AUV bathymetry from 2009, **(b)** post-eruption *Sentry* AUV bathymetry from 2017, **(c)** positive depth differences between the AUV surveys (after the 2017 *Sentry* AUV grid was co-registered by shifting it 8 m east and 16 m south), and **(d)** trackline of *SuBastian* ROV dive S86 (white line) on post-eruption *Sentry* AUV bathymetry, with locations of images in **Figure 6** (white numbered circles). Part of *SuBastian* ROV dive S103 also crossed this area, but is not shown in **(d)**. In **(c)** note that shingled lava plateaus thicken downslope away from the rift zone (see text for discussion). Black outlines enclose the site #1 eruption deposits and mark the edges of individual shingled lava plateaus.

based on the fact that most pillows are buried and only the largest poke above the tephra (**Figure 6f**). The tephra layer is pock-marked by numerous bowl-shaped, circular pits, about 0.5–1 m across (**Figures 6e,f**) that apparently formed when tephra "drained" downward into empty cavities among the underlying pillow lavas. Locally, these circular pits have accumulated small yellow flocculent particles of microbial mat (**Figure 6f**), which apparently originally formed on the upper surface of the tephra, but were subsequently dislodged and transported into the pits by bottom currents. Locally, a mosaic of white and yellow microbial mat still blanketed the tephra in some areas (**Figure 6g**). We measured a temperature of 5°C (a few degrees above ambient) in one such area with the ROV's temperature probe as it was pushed downward about 10 cm into the tephra deposit. The steps between the lava plateaus are constructional levees of nearly vertical pillow lava tubes, and were relatively unburied by tephra because of their steepness (**Figure 6h**).

Site 2: The 2012–2016 Eruption East of the Summit at 1300 mbsl

The first of the three eruption sites constrained in time between 2012 and 2016 is located on the uppermost ENE rift zone just east of the summit (**Figure 7**). The shallowest point at the eruptive vent is 1255 mbsl and the deepest extent of the erupted deposits is at least 1950 mbsl on both the SE and N flanks of the rift zone. The area and volume of the 2011–2016 depth differences from this eruption are 0.53×10^6 m^2 and 13.8×10^6 m^3, respectively (**Table 2**).

Figure 8 shows a smaller area near the summit and eruptive vent in more detail. The 2009–2017 time period between the two AUV surveys captures changes due to several events during that span. A new pit crater formed at the summit between December 2010 and November 2011 when the area that included the Hades and Prometheus vents collapsed (**Figures 8a,b**), perhaps associated with the end of continuous eruptive activity (Embley et al., 2014). The crater has a roughly oval outline, about 200 × 100 m wide and 100 m deep, with the long axis parallel the rift zones (**Figure 8c**). The crater rim on the NW edge displays elongated pillow lava lobes, probably originally fed from Hades vent but now truncated by the collapse (see Figures 10c,d of Embley et al., 2014). The deepest part of the crater (1290 mbls), just 25 m W of the former location of Hades vent, hosted diffuse venting of clear shimmering fluids up to 22°C in 2017. The former location of Hades is now a high-standing pinnacle within the crater, and the former location of Prometheus vent is along the eastern rim of the crater (**Figure 8c**), where it abuts the east-facing headwall of the landslide that also occurred between December 2010 and November 2011 (Embley et al., 2014). The high-standing areas remaining between Hades and Prometheus may have escaped significant collapse (**Figure 8**), perhaps because the former vent areas are underlain by relatively massive intrusive rocks. These are also areas of continuing extensive diffuse hydrothermal venting.

The 2012–2016 eruptive vent is 70 m below and 300 m east of the summit, and was clearly centered within the headwall scar of the 2010–2011 landslide (labeled in **Figure 8c**), where

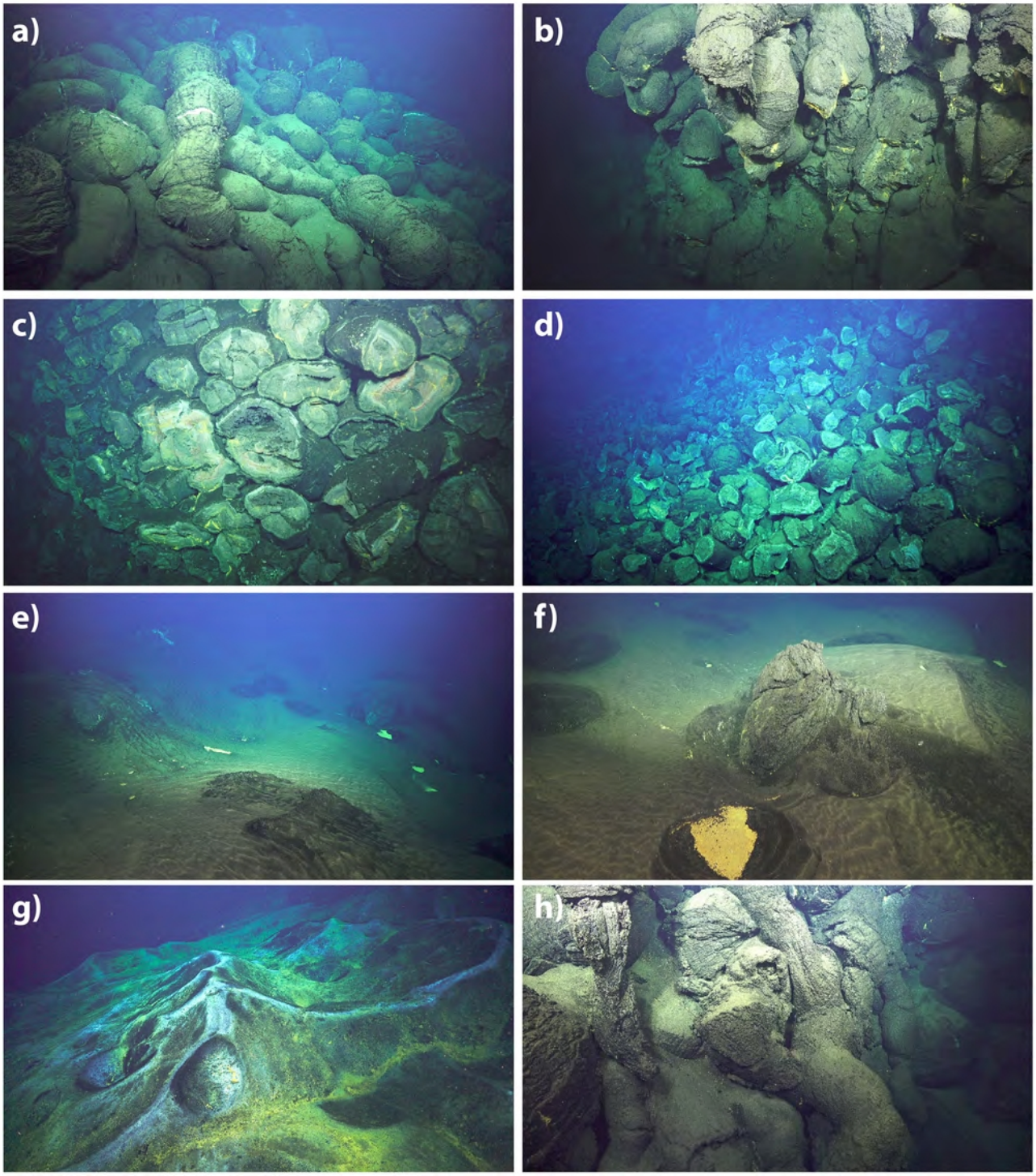

FIGURE 6 | Images of eruption site #1 from ROV *SuBastian* dive S86. All are 2016–2017 eruption products. Numbers in parentheses are time of photo in GMT and horizontal scale. See **Figure 5d** for photo locations. **(a)** Pillow lavas on the slope below the rift zone (19:17:22, 5 m). **(b)** Nearly vertical cliff face of intact pillow lavas (20:09:42, 4 m). **(c)** Nearly vertical cliff of truncated pillows on the headwall of a landslide scarp (20:52:51, 4 m). **(d)** Talus with pillow fragments below a landslide scarp (20:48:50, 10 m). **(e)** Tephra-covered pillow lavas on a shingled lava plateau near the eruptive fissures, with circular pits containing yellow microbial floc in the distance (21:40:18, 10 m). **(f)** Closer view of collapse pit in tephra deposit with yellow microbial floc (bottom) and large partially buried pillow at center (21:47:06, 4 m). **(g)** Colorful microbial mats growing on tephra completely burying pillow lavas on a shingled lava plateau near the eruptive fissures (23:41:48, 6 m). **(h)** Exposed tubular pillow lavas on the steep step between shingled lava plateaus (22:27:47, 3 m).

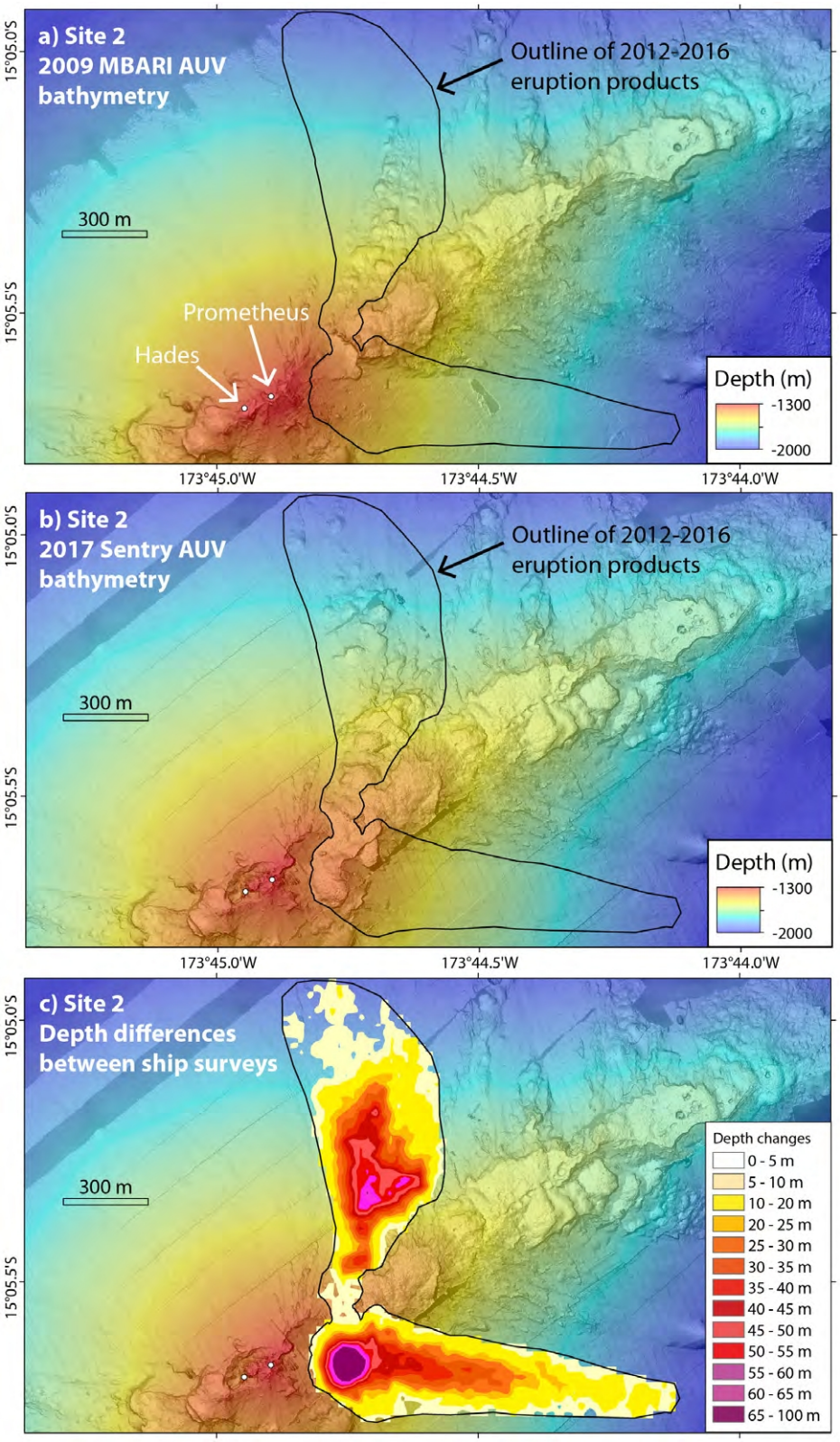

FIGURE 7 | Broad-view maps of eruption site #2, just east of the summit of West Mata (see **Figure 2**) showing **(a)** pre-eruption MBARI AUV bathymetry from 2009, **(b)** post-eruption *Sentry* AUV bathymetry from 2017, and **(c)** positive depth differences between ship-based surveys in 2012 and 2016 (**Table 2**). Black outlines enclose the site #2 eruption deposits. White dots show locations of Hades and Prometheus eruptive vents in May 2009.

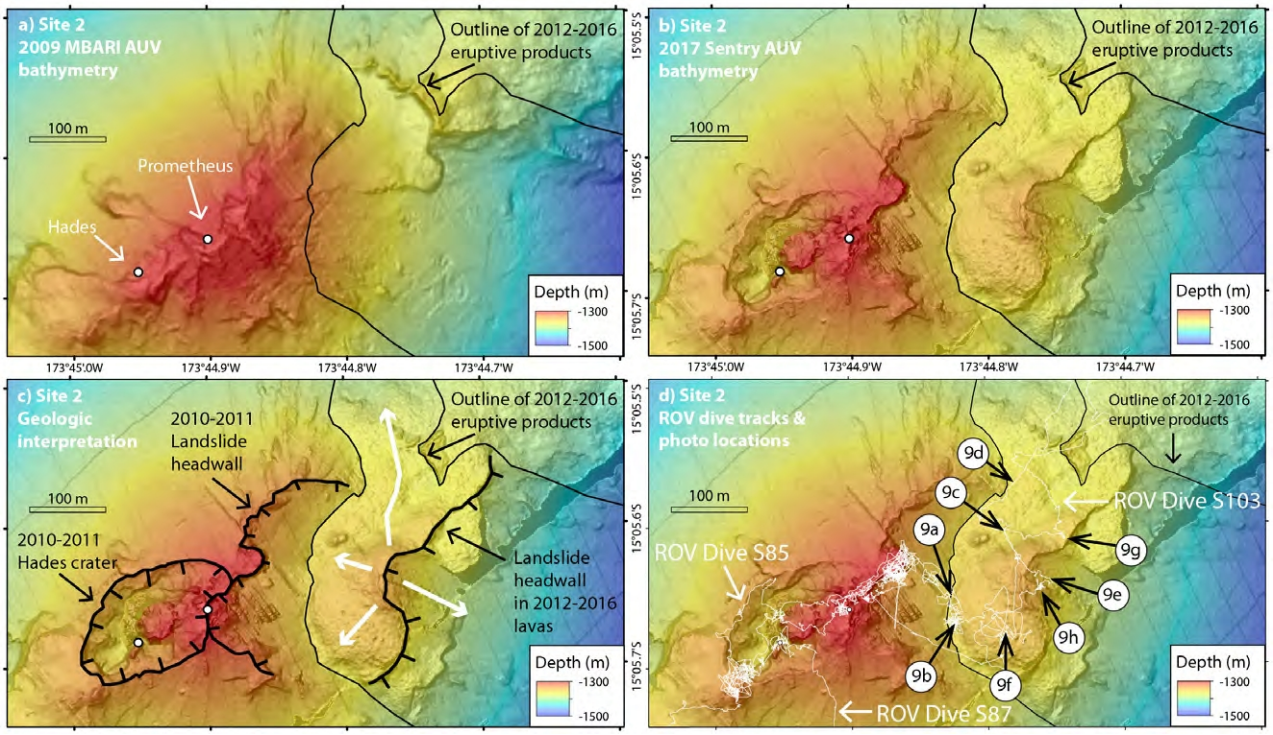

FIGURE 8 | Close-up maps of eruption site #2 showing **(a)** pre-eruption MBARI AUV bathymetry from 2009, **(b)** post-eruption *Sentry* AUV bathymetry from 2017, **(c)** geological interpretation on 2017 AUV bathymetry and **(d)** tracklines of *SuBastian* ROV dives S85, S87, and S103 (white lines) on post-eruption *Sentry* AUV bathymetry, with locations of images in **Figure 9** (white numbered circles). Thick white arrows in **(c)** indicate lava flow directions from eruptive vent; thick black hachured lines are crater rims or landslide headwalls. Thin black outlines enclose the site #2 eruption deposits. White dots show locations of Hades and Prometheus eruptive vents in May 2009.

the new lavas are shallowest and the largest depth differences (up to 93 m) form a circular bullseye pattern (**Figure 7c**). From there, it appears that lava and clastic debris were first deposited downslope to the east >1 km, more or less down the axis of the previous landslide chute, but as the eruption built a constructional mound over the vent, it gained enough elevation to also feed pillow lava flows down the northern flank of the rift zone (**Figure 8c**). The thickest accumulation of lava on the north side of the rift (67 m) is mid-way down the flank (**Figure 7c**). The morphology of the downslope eruptive deposits are notably different on the two sides of the rift zone; on the SE side they are smooth, whereas those on the N side are hummocky (**Figure 7b**). This contrast indicates the early deposits on the SE side are mainly volcaniclastic, suggesting more explosive or higher-effusion rate activity at the beginning of the eruption, whereas those on the north are intact pillow lava flows, suggesting the later phase of the eruption developed a more stable lava distribution system from the vent to the north slope, perhaps at a lower effusion rate. On the axis of the rift zone, the depth differences are relatively thin (4–11 m, **Figure 7c**), but it is clear there is new lava there because of different morphology in the 2017 AUV bathymetry (**Figure 8b**) and our ROV dive observations. Nevertheless, there are some older high-standing features in that area that did not get buried by the new lava flows. The 2017 AUV bathymetry also shows that the 2012–2016 lava flows are themselves cut by east-facing landslide scarps on the south side of the rift zone (**Figure 8c**). These appear to have formed both during and after the eruption since there are some pillow-lava deposits on the slope below the landslide headwall (**Figure 8c**).

ROV *SuBastian* dives S85, S87, and S103 were made in this area (**Figure 8d**) and showed that the near-vent deposits are pillow lavas that form a steep flow front where they abut the 2010–2011 landslide headwall west of the eruptive vent (**Figures 9a,b**). As the eruptive vent was approached, thick deposits of tephra were observed mantling the pillows (**Figure 9c**), and were locally covered by white and yellow microbial mats (**Figure 9d**). Near the eruptive vent spatter-like deposits were observed (**Figure 9e**) providing more evidence for a pyroclastic component to the eruption. Diffuse venting of clear hydrothermal fluids was observed over a large area that was colonized by abundant vent animals including shrimp, squat lobsters, and polychete worms (**Figure 9f**). The edge of the pillow mound that had been cut by a landslide was marked by truncated pillows, some of which were hollow with drained-out interiors (**Figure 9g**). Within the landslide headwall, cross-sections of the pillow mound could be seen in near-vertical outcrops oriented downslope, showing layer upon layer of elongate pillows (**Figure 9h**).

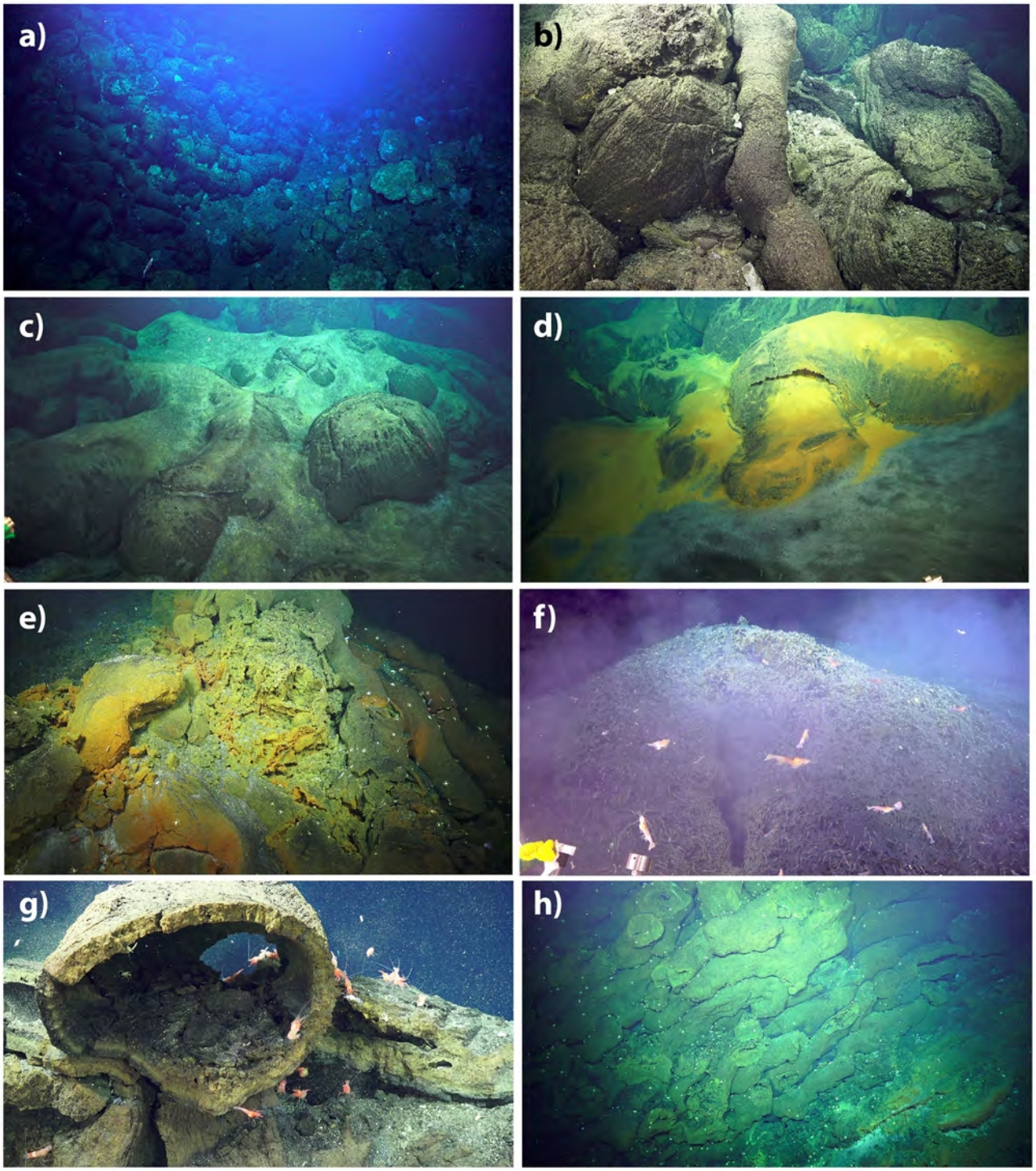

FIGURE 9 | Images of eruption site #2 from ROV *SuBastian* dives S85, S87, and S103. All show 2012–2016 eruption products. Numbers in parentheses are dive number, time of photo in GMT and horizontal scale. See **Figure 8d** for photo locations. **(a)** 2012–2016 flow front at left against the 2010–2011 landslide headwall at right (S85, 01:52:19, 10 m). **(b)** Close up of pillow lavas on flow front (S85, 01:58:13, 3 m). **(c)** Tephra partly burying pillows close to eruptive vent (S85, 02:59:14, 5 m). **(d)** Tephra with white and yellow microbial mats mantling pillows (S85, 03:18:12, 3 m). **(e)** Near-vent spatter deposits with yellow hydrothermal sediment (S85, 02:50:48, 5 m). **(f)** Hydrothermal vent shrimp swarm at active diffuse vent with shimmering cloudy water (S87, 03:19:25, 3 m). **(g)** Hollow drained-out pillow where new lavas are cut by landslide scarp (S103, 02:42:53, 1.5 m). **(h)** Cross-section of stack of elongate pillow lavas cut by landslide scarp, with downslope direction to the left (S85, 02:45:15, 10 m).

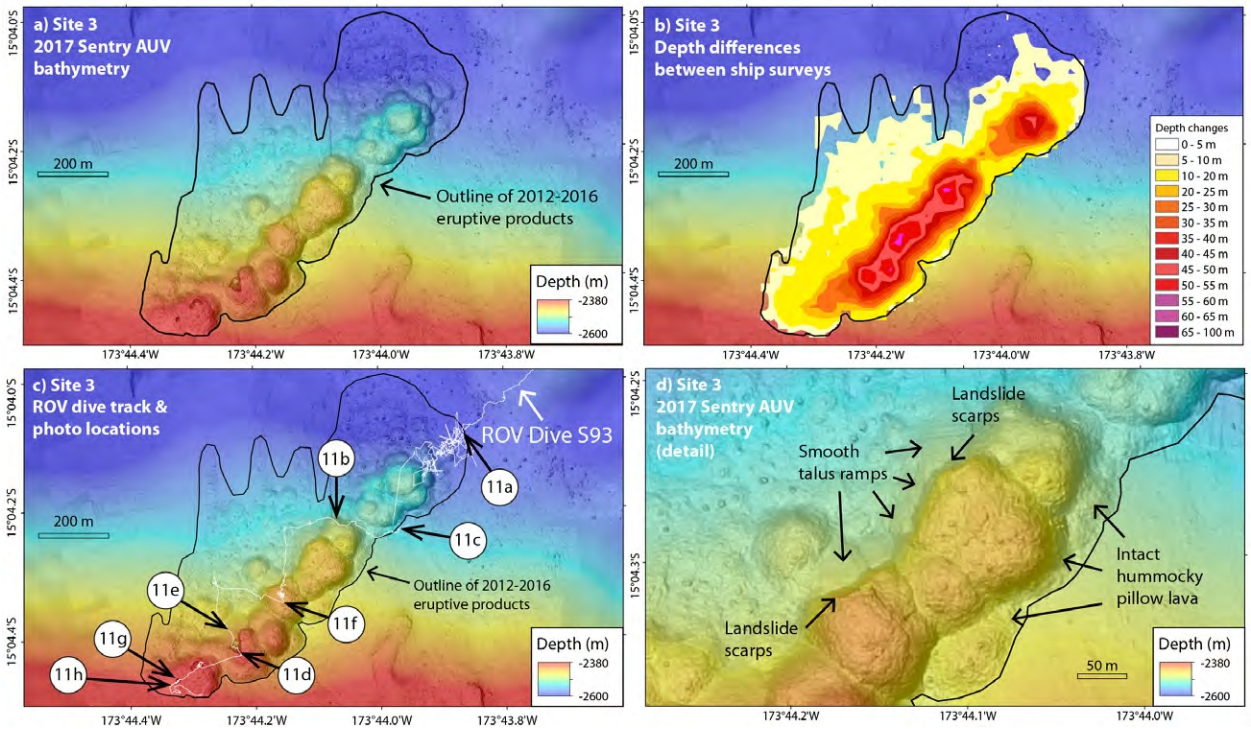

FIGURE 10 | Maps of eruption site #3, the pillow ridge on the NE flank of West Mata (see **Figure 2**) showing **(a)** post-eruption *Sentry* AUV bathymetry from 2017, **(b)** positive depth differences between ship-based surveys in 2012 and 2016 (**Table 2**), **(c)** trackline of *SuBastian* ROV dive S93 (white line) on *Sentry* AUV bathymetry, with locations of images in **Figure 11** (white numbered circles), and **(d)** close-up showing hummocky intact pillow lavas on the gentler upslope side of the ridge contrasting with smooth talus ramps below landslide scarps on the steeper downslope side. Black outlines enclose the site #3 eruption deposits.

Site 3: The 2012–2016 Eruption on the NE Flank at 2400 mbsl

The second recent eruption site constrained in time between 2012 and 2016 is located on the NE flank of West Mata (**Figure 2**). It is unusual because it is well off the ENE rift zone and the smooth morphology of the rest of the NE flank (from volcaniclastic debris produced upslope) makes it clear that eruptions do not occur here often. This site was beyond the coverage of the 2009 AUV survey, so we do not have high-resolution bathymetry before the eruption, but pre-2012 ship-based bathymetry shows a featureless slope. The post-eruption AUV survey in 2017 (**Figure 10a**) shows that the eruption produced a linear ridge of coalesced pillow lava mounds that is rotated ∼26°clockwise to the radial direction from the summit. The orientation of the pillow ridge may have been influenced by basement structure nearby, as it is parallel to an older sedimented and tectonized ridge NE of the volcano (**Figure 2**). Lava was apparently erupted along a fissure ∼1 km long, extending from 2365 to 2635 mbsl on a slope averaging 15–20°. The depth differences between ship-based surveys (**Figure 10b**) show the maximum thickness of the lavas is 57 m, the area of erupted material is 0.25×10^6 m^2, and the volume is 6.7×10^6 m^3 (**Table 2**).

ROV *SuBastian* dive S93 traversed from the NE base of the volcano upslope along the length of the 2012–2016 pillow ridge (**Figure 10c**). The hummocky areas of lesser depth change that extend as fingers downslope from the thick pillow ridge (**Figures 10a,b**) are thinner (<10 m) flows of pillow lava. These were apparently produced in an early phase of the eruption when lava was fed from the fissure at a slightly higher effusion rate before it slowed and became localized at discrete points along the eruptive fissure to produce the thicker pillow mounds. The thinnest margins of the flow field (probably the earliest flows) are covered with rippled deposits of tephra (**Figure 11a**), suggesting downslope transport by turbidity currents during a pyroclastic phase of this eruption. Deposits of tephra are ubiquitous on the thicker pillow lavas, but are less obvious on steeper slopes. On the upslope sides of the pillow mounds, the constructional slopes are nearly vertical (**Figure 11b**) with elongate pillow lava tubes that remained intact all the way to the flow margins (**Figure 11c**). In contrast, on the unbuttressed downslope sides of the pillow mounds, the pillow lavas did not remain intact and formed vertical cliffs of truncated pillows in the upper reaches (**Figure 11d**) and aprons of pillow talus below (**Figure 11e**). This contrast in morphology is evident in the high-resolution AUV bathymetry with intact hummocky flows on the upslope side of the pillow mounds, and cliffs with smooth ramps of pillow talus below on the downslope side (**Figure 10d**). On the flatter tops of the pillow mounds, a thin dusting of yellow sediment (**Figure 11f**) and abundant polychete worms were evidence for

low-level diffuse hydrothermal venting. The tops of the uppermost pillow mounds are marked by small pit craters (**Figure 10a**) with overhanging edges (**Figure 11g**), indicating that some of the mounds had a core of molten lava that drained out and collapsed during the later stages of the eruption. Locally, the tops of the pillow mounds were covered with pyroclastic tephra deposits up to several 10s of cm thick, with occasional collapse pits as seen at site #1 (**Figure 11h**).

Site 4: The 2012–2016 Eruption at the NE Base at 2650 mbsl

The third of the recent eruption sites between 2012 and 2016 is also in an unusual location, at the NE base of the volcano in a basin 1–2 km north of the axis of the deepest part of the ENE rift zone (**Figure 2**). Before the eruption, ship-based bathymetry showed a broad oval basin in the area, 1–1.5 km across and relatively flat at ∼2700 mbsl. The 2009 AUV survey did not extend over this site. After the eruption, ship-based bathymetry shows positive depth changes throughout the basin up to 64 m (**Figure 12b**), covering an area of 0.73×10^6 m^2, and amounting to a volume change of 17.1×10^6 m^3 (**Table 2**).

The AUV bathymetric survey over this site in 2017 was particularly revealing (**Figure 12a**). The high-resolution map showed that much of the eastern half of the basin appeared to be uplifted sediments (**Figure 12c**), smooth seafloor that had been domed upward and cut by numerous longitudinal spreading cracks, like those on a loaf of bread when it comes out of the oven (suggesting a nickname we used for the site: "the muffin"). The uplifted sediments were surrounded by hummocky seafloor that appeared to be young lava flows that flowed around the uplift without a clearly defined eruptive vent (**Figure 12c**).

Observations during ROV *SuBastian* dive S88 confirmed this interpretation (**Figure 12d**). The edges of the young lava flow are marked by thin pillow lobes over the surrounding sediment, with occasional larger higher-standing pillows that have undergone inflation, expansion, and cracking (**Figure 13a**). The new lavas and the surrounding sediments are both covered with volcaniclastic-rich ripple marks that form a zebra-striped polygonal pattern with darker tephra on the ripple crests and lighter-colored pelagic sediment in the troughs (**Figures 13a–d**). The volcaniclastic-rich sediment is about 1–2 cm thick on the young lavas and appears to be evenly distributed throughout the area (on both sediments and lava), with no locally thicker accumulations observed. Because of this, we interpret that the majority of volcaniclastic material is not juvenile (syn-eruptive). Instead, we hypothesize that it was probably deposited by turbidity currents from further upslope after the eruption, such as those documented by Walker et al., under review[3]. This interpretation implies that pyroclastic tephra was not a major component of the eruptive products at this site, the deepest of the four most recent eruption sites (2650–2700 mbsl).

A series of sinuous tumulus structures, up to 125 m long and 5 m high are located between the two areas of uplifted sediment in the AUV bathymetry (**Figure 12c**). Tumuli are formed by internal pressure within inflating lava flows that pushes up the overlying solidified crust in a trap-door fashion on either side of an axial crack (Walker, 1991; Appelgate and Embley, 1992). These tumuli are the shallowest features on the 2012–2016 lava flows (**Figure 13e**), and are in line with the long-axis of the large dome of uplifted sediment, so may overlie the eruptive vents for the lava flows. From there, pillow lavas flowed mostly to the west and then northward, around the uplifted sediment, but also flowed a shorter distance to the east (**Figure 12c**). North of the tumuli, the young lavas lap up onto the uplifted dome of sediment (**Figure 13f**). The longitudinal cracks on the sediment dome that are evident in the AUV bathymetry appear as broad swales, 10–40 m wide and 3–8 m deep, with little or no stratigraphy evident in their walls in the southern half of the dome (**Figure 13g**). However, in the center of the uplifted sediment dome, where the swales are wider and deeper, stratigraphy was exposed in the side walls and yellow microbial mat showed evidence of local diffuse hydrothermal discharge (**Figure 13h**). At that site the ROV's temperature probe measured a temperature of 15°C within the sediments, apparently residual heat from magma intruded below.

Site 5: The 2010–2011 Eruption on the Deep WSW Rift at 2950 mbsl

In December 2017, we also made ROV *SuBastian* dive S95 on two older areas of depth change (sites #5–6, **Figure 2**) documented on the deep WSW rift zone by Embley et al. (2014). These are the first visual observations of these eruption sites and provide ground-truth that these depth changes are indeed associated with young lava flows. They also give additional information on the character of recent eruptions at West Mata, particularly at the deepest depths.

The first of the two eruption sites (site #5) visited on ROV dive S95 (**Figure 14c**) is constrained in time between May 2010 and November 2011 (time period IV + V of Embley et al., 2014). Because this area is beyond the obvious morphological extent of the rift zone, it was not mapped during the 2009 AUV bathymetric survey. We attempted to map the site with AUV *Sentry* in 2017, but unfortunately the multibeam sonar failed on this dive (#463) and so no high-resolution bathymetry exists for this site (although a photo survey was collected by *Sentry*). The post-eruption ship bathymetry (**Figure 14a**) and the 2010–2011 depth differences (**Figure 14b**) show that the lava flows that were erupted cover an area of 1300 by 700 m across (0.61×10^6 m^2), are up to 63 m thick along a ridge oriented ENE-WSW in the southern half of the flow field (probably overlying the eruptive fissure), and have a total volume of 16.0×10^6 m^3 (Embley et al., 2014).

The lava flow field is composed entirely of intact lava flows, with no landslide scarps or talus ramps, due to the relatively low slopes that existed in this area before the eruption. The lavas have a fine dusting of light-colored sediment on them. The northern margin of the lava flow field has broad pillow lava lobes (**Figure 15a**), which grade locally into lobate and ropy sheet flow morphology, in some areas with very flat

[3]Walker, S. L., Baker, E. T., Lupton, J. E., and Resing, J. A. (under review). Patterns of fine ash dispersal related to volcanic activity at West Mata volcano, NE Lau Basin. *Front. Mar. Sci.*

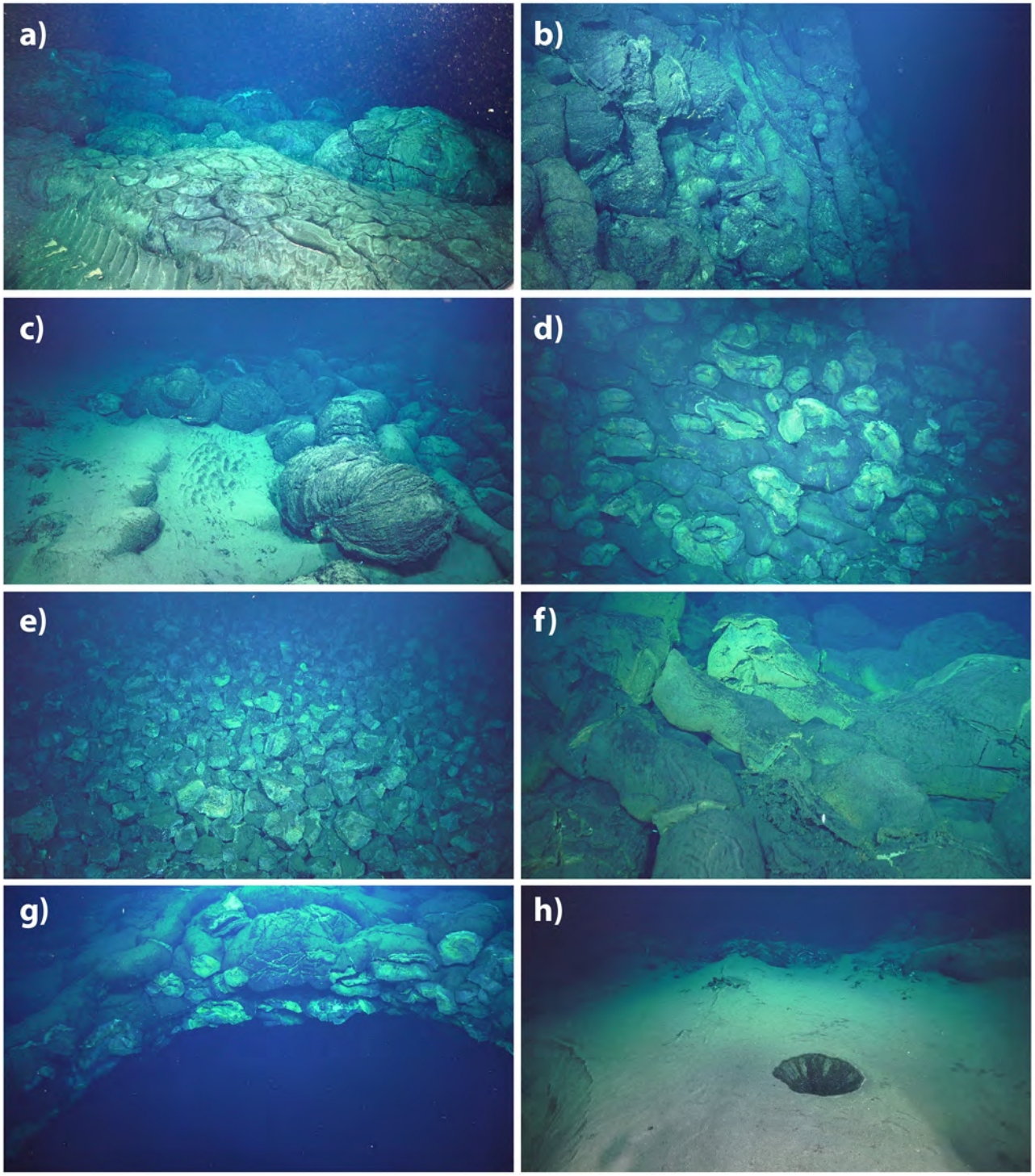

FIGURE 11 | Images of eruption site #3 from ROV *SuBastian* dive S93. All show 2012–2016 eruption products. Numbers in parentheses are time of photo in GMT and horizontal scale. See **Figure 10c** for photo locations. **(a)** Rippled tephra-rich sediment deposited on thin pillow lava flow margin downslope of pillow ridge (21:26:05, 5 m). **(b)** Nearly vertical constructional slope on upslope side of pillow ridge (23:19:35, 5 m). **(c)** Margin of young lavas (at right) on upslope side of pillow ridge (22:48:40, 4 m). **(d)** Truncated pillows in landslide scarp on steeper downslope side of pillow ridge (01:39:25, 8 m). **(e)** Ramp of pillow talus below landslide scarp on downslope side of pillow ridge (01:33:28, 10 m). **(f)** Thin yellow hydrothermal sediment and tephra on lavas at top of pillow ridge (00:32:02, 3 m). **(g)** Overhanging rim of collapse pit at top of pillow mound due to drain-out of molten interior (02:33:15, 4 m). **(h)** Tephra deposit mantling pillow lavas at upslope end of pillow ridge (02:48:08, 5 m).

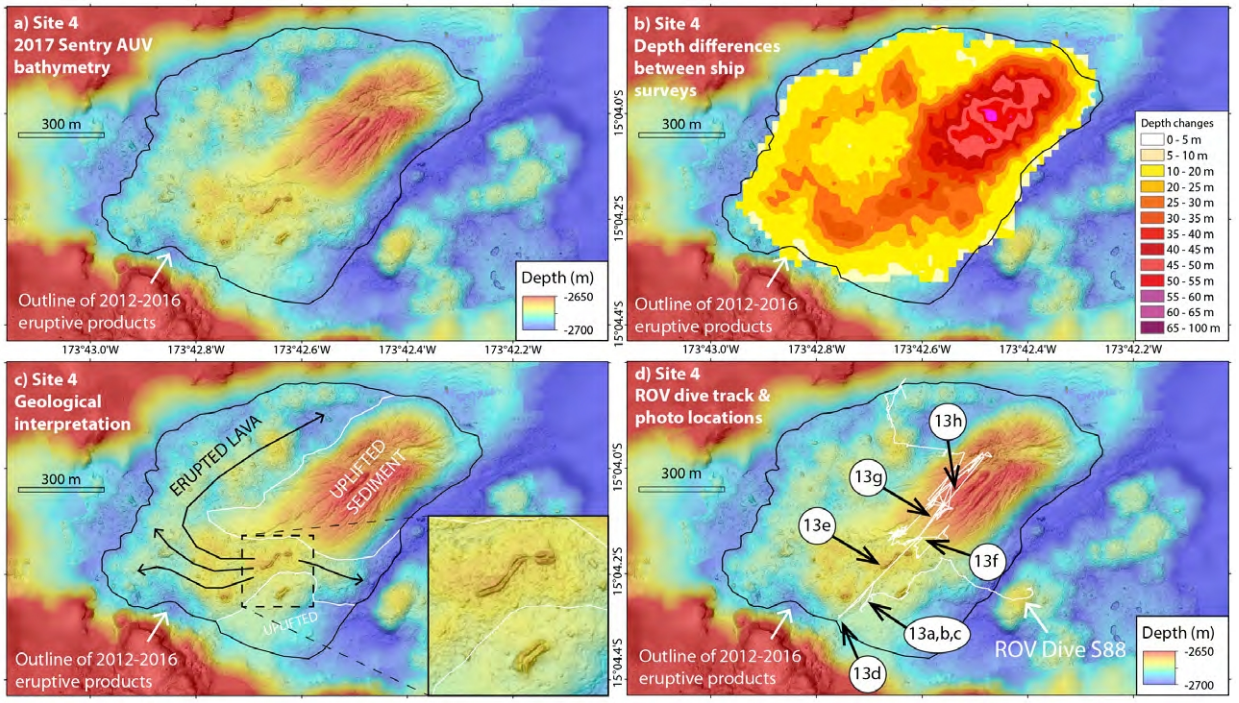

FIGURE 12 | Maps of eruption site #4, at the NE base of West Mata (see **Figure 2**) showing **(a)** post-eruption *Sentry* AUV bathymetry from 2017, **(b)** positive depth differences between ship-based surveys in 2012 and 2016 (**Table 2**), **(c)** geological interpretation on 2017 AUV bathymetry, and **(d)** trackline of *SuBastian* ROV dive S88 (white line) on *Sentry* AUV bathymetry, with locations of images in **Figure 13** (white numbered circles). In **(d)** note that the navigation for this dive was considerably noisier than for others on this expedition due to problems with the acoustic tracking system on *R/V Falkor*. Black outlines enclose the site #4 eruption deposits; white outlines in **(c)** delineate uplifted sediments and inset shows detail of tumuli structures in young lava flows.

upper surfaces that are locally uplifted into tumuli structures (**Figure 15b**), providing evidence for flow inflation. Further south, long tubular pillows mantle the northern slope of the ENE-WSW eruptive ridge (**Figure 15c**). Near the crest of that ridge, the pillows again broadened on the gentler slope, and sheet-like lava morphology with local drainback were observed near an apparent eruptive fissure (**Figure 15d**). On the north side of the flow field where it sloped down and abutted a sedimented ridge, tephra-rich ripple marks in the sediment were oriented perpendicular to the axis of the rift zone with volcaniclastic accumulations on the lee sides (**Figure 15e**), consistent with sediment transport from further upslope by bottom currents. No significant accumulations of tephra were observed on the 2010–2011 lava flows. This is the deepest of the recent eruption sites (2890–2975 mbsl).

Site 6: The 1996–2008 Eruption on the Deep WSW Rift at 2750 mbsl

On the same ROV dive (*SuBastian* S95) we also traversed the eruption site that is just upslope on the WSW rift zone (site #6, **Figure 2**), which was discovered and constrained between the 1996–2008 bathymetric surveys by Embley et al. (2014) (their time period I). In contrast to the previous site, this eruption was on the deepest morphologic expression of the WSW rift zone and so was included in the 2009 AUV bathymetric survey, which is a post-eruption survey in this case (**Figure 14a**). The depth differences between the ship-based surveys in 1996 and 2008 are up to 101 m (**Figure 14b**), with an area of 0.22×10^6 m^2 and a volume of 12.0×10^6 m^3 (Embley et al., 2014).

The morphology of this site is considerably different than the previous one, mostly because the eruption occurred on the much steeper slopes on the rift zone. Consequently, the flow field is composed of repeated sequences of gently sloping intact pillow lavas on the crests of constructional mounds (**Figure 15f**), surrounded by steep slopes of truncated pillows on the margins of the mounds (**Figure 15g**), where the pillows have broken apart and formed talus ramps below (**Figure 15h**), which in turn lap onto the next constructional pillow mound downslope (**Figure 14**). Again, no significant tephra accumulations were observed on these lava flows. Neither site #5 or #6 displayed any evidence of active hydrothermal venting (shimmering water, microbial mats, vent animals, etc.), but local accumulations of yellow hydrothermal sediment showed that it had occurred previously.

DISCUSSION

Comparison of Recent Eruption Sites

The most recent ROV dive observations show that all four of the most recent eruption sites at West Mata (#1–4; 2012–2018)

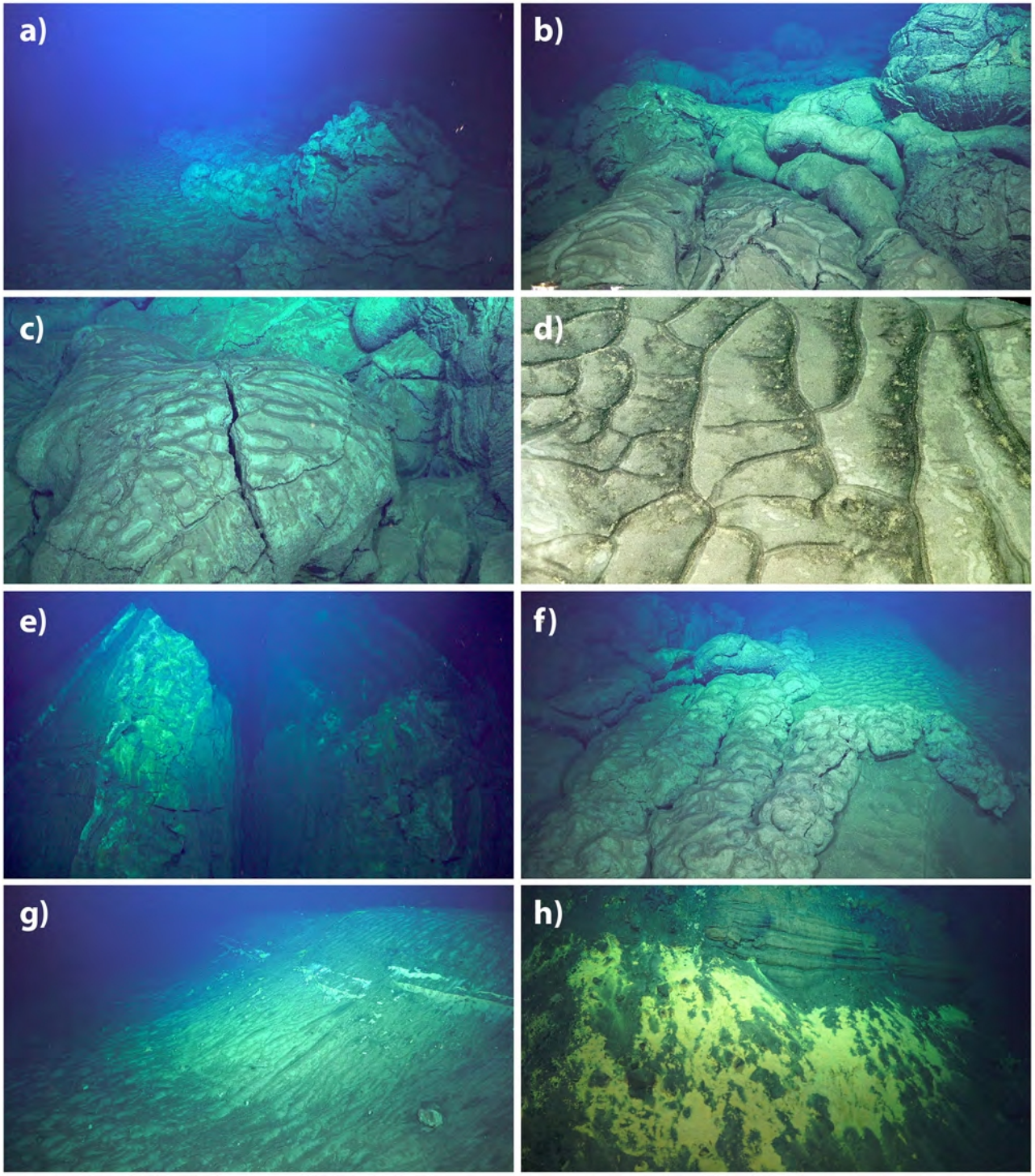

FIGURE 13 | Images of eruption site #4 from ROV *SuBastian* dive S88. Numbers in parentheses are time of photo in GMT and horizontal scale. See **Figure 12d** for photo locations. **(a)** Margin of 2012–2016 pillow lavas at right (21:32:51, 8 m). **(b)** Closer view of 2012–2016 pillow lavas (21:11:48, 3 m). **(c)** Lava lobe with rippled volcaniclastic-rich sediment on surface (21:05:22, 2 m). **(d)** Close up of rippled volcaniclastic-rich sediment (21:47:26, 0.5 m). **(e)** Uplifted lava at tumulus structure (23:18:54, 8 m). **(f)** 2012–2016 pillow lava (left) lapped up on south edge of uplifted sediment dome at right (23:50:51, 3 m). **(g)** Broad swale (left) and edge of extension crack (right) in southern part of uplifted sediment dome (00:32:58, 10 m). **(h)** Yellow microbial mat growing on edge of extensional crack with stratigraphy in central part of uplifted sediment dome (00:35:18, 5 m).

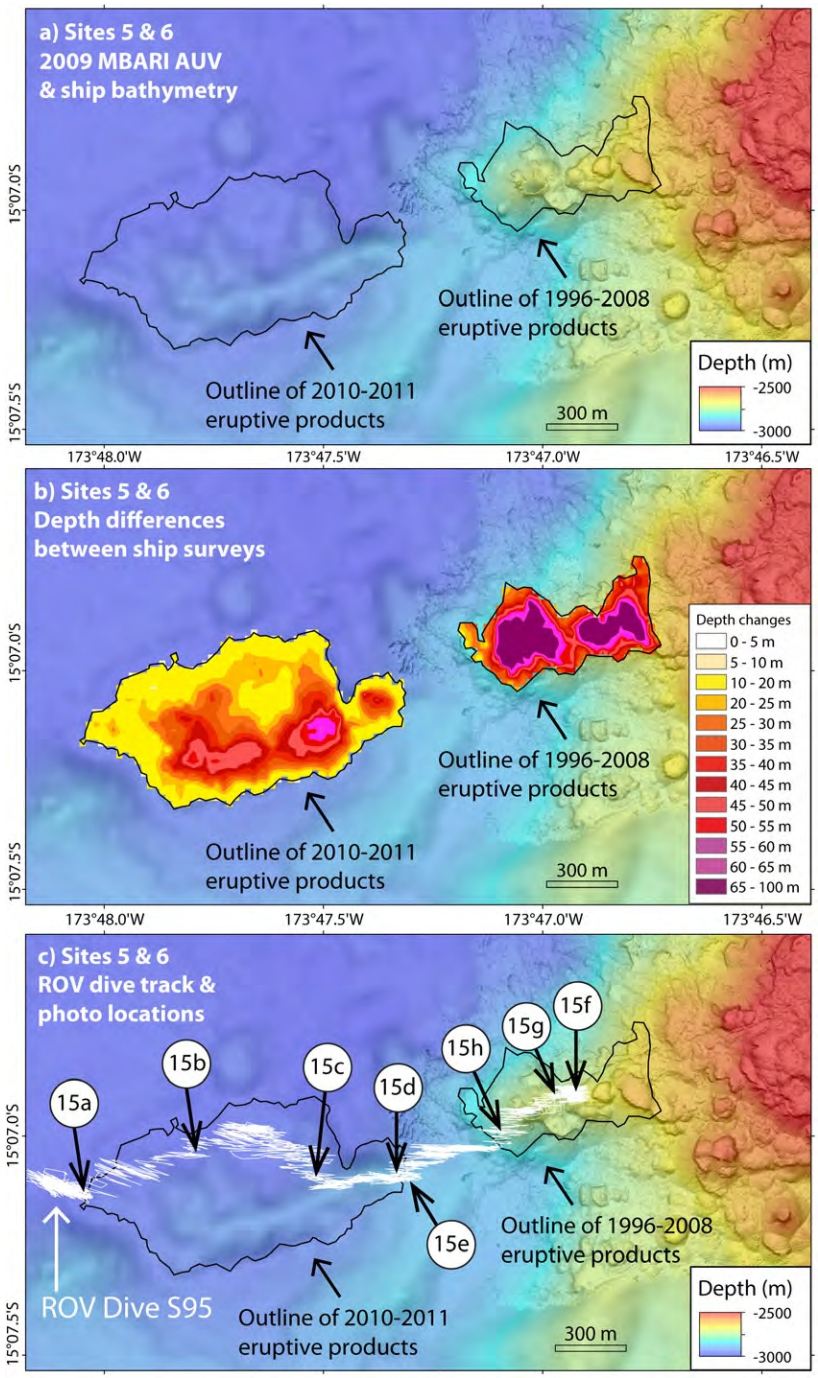

FIGURE 14 | Map of eruption sites #5 (left) and #6 (right), at the SW base of West Mata (see **Figure 2**) showing **(a)** post-site-#5-eruption ship-based bathymetry (left) overlain with post-site-#6-eruption MBARI AUV bathymetry from 2009 (right), **(b)** positive depth differences between ship-based surveys (2010–2011 at left, 1996–2008 at right, see **Table 2**), and **(c)** trackline of *SuBastian* ROV dive S95 (white line) on post-eruption bathymetry, with locations of images in **Figure 15** (white numbered circles). Note that the navigation for this dive was considerably noisier than for others on this expedition due to problems with the acoustic tracking system on *R/V Falkor*. Black outlines enclose the site #5 and #6 eruption deposits.

have deposits that were still warm and cooling in December 2017 (from months to perhaps up to 5 years after they were erupted), exhibiting some combination of diffuse hydrothermal venting colonized by vent animals (particularly shrimp, squat lobsters, and polychetes), microbial mats, and elevated temperatures measured in tephra or sediments just below the surface. In addition, diffuse hydrothermal venting was observed all around the summit, both inside and outside of Hades Crater, despite

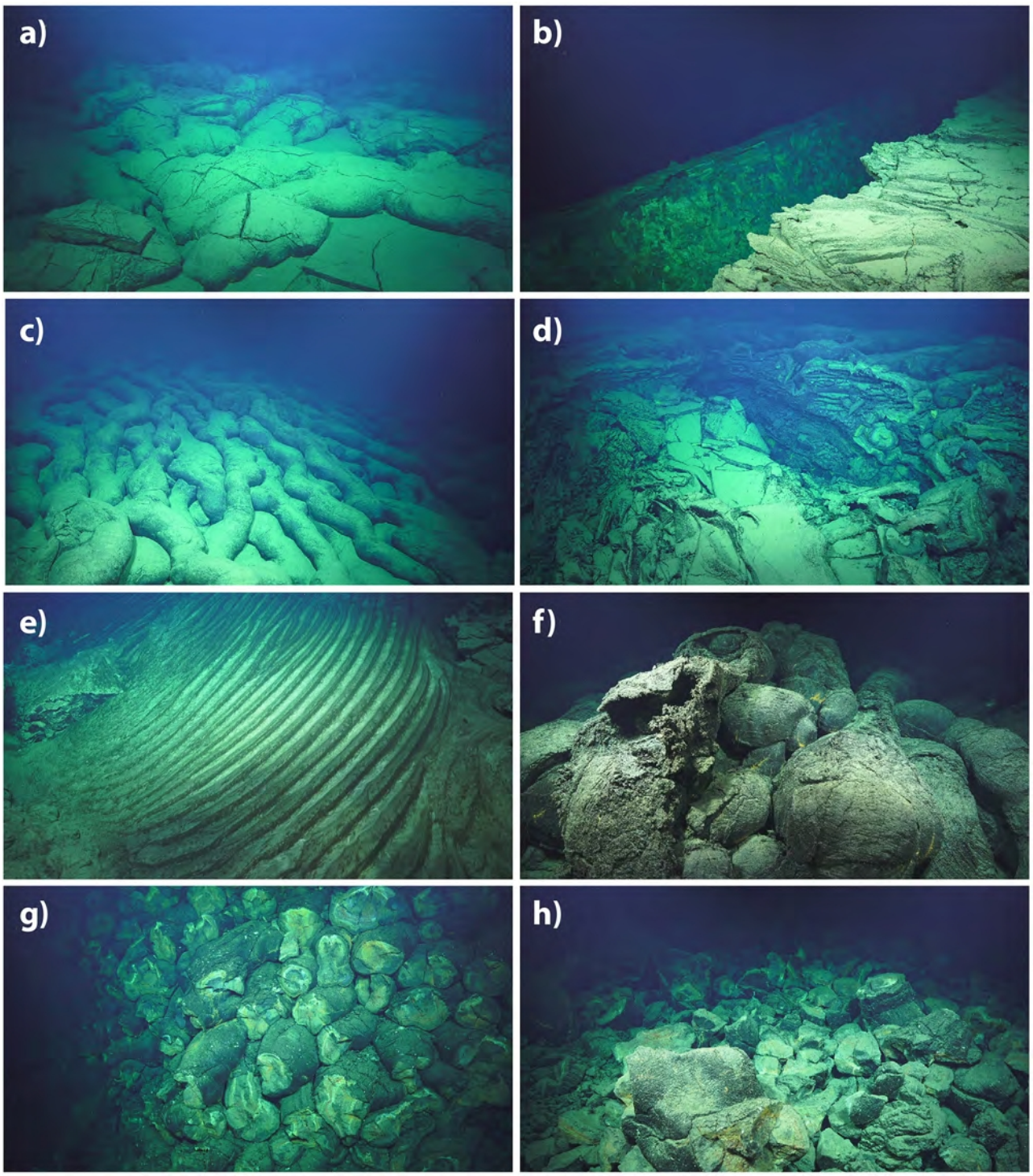

FIGURE 15 | Images of eruption sites #5 (2010–2011) and #6 (1996–2008) from ROV *SuBastian* dive S95. Numbers in parentheses are time of photo in GMT and horizontal scale. See **Figure 14c** for photo locations. **(a)** Broad lobes of 2010–2011 lava near northern flow margin (20:34:50, 5 m). **(b)** Uplifted sheet lava in tumulus structure near northern 2010–2011 flow margin (22:21:14, 5 m). **(c)** elongate pillows on north slope of 2010–2011 pillow ridge (23:14:48, 8 m). **(d)** Eruptive fissure with lava drain-out at crest of 2010–2011 pillow ridge (01:24:04, 8 m). **(e)** Volcaniclastic-rich sediment ripples at southern margin of 2010–2011 pillow ridge, oriented perpendicular to the downslope direction (00:05:08, 5 m). **(f)** Crest of 1996–2008 pillow lava mound with intact lavas (03:35:11, 3 m). **(g)** Landslide scarp of truncated 1996–2008 pillows on downslope edge of pillow mound (03:31:13, 5 m). **(h)** Pillow talus below landslide scarp in 1996–2008 lavas (02:39:27, 5 m).

the end of eruptive activity there by early 2011. This implies that active diffuse hydrothermal activity exists more or less continuously at West Mata due to the heat delivered or mined from recent eruption sites and the relatively short recurrence interval between eruptions. This is important for the continuity of local vent-dependent ecosystems. In contrast, no evidence for continued venting was observed at the two older eruption sites visited by ROV in 2017 (#5–6; 1996–2011), suggesting that venting usually does not persist for longer than 5–10 years at eruption sites on the rift zones.

The ROV dive observations also show that there is a variation in eruptive character with depth at West Mata. The shallower recent eruption sites (sites #1, #2, and to some extent #3) have very significant deposits of tephra near the eruptive vents (up to 1–2 m thick and extending for 100s of m laterally), showing that violent degassing and lava fragmentation are common. We envision this eruptive behavior as similar to the spectacular video observations of explosive activity at the summit vents during ROV *Jason* dives in May 2009 (Resing et al., 2011; Rubin et al., 2012). In addition, there is some evidence that the eruptive style evolves during a single eruption, with a progression from more pyroclastic to more effusive with time. On the other hand, at site #1 a thick tephra deposit overlies pillow lavas, so it appears that pyroclastic activity continued throughout the eruption there. In contrast, the deeper recent eruption sites (sites #4, #5, and #6) do not have locally thick, near-vent deposits of tephra, suggesting that little tephra is produced by eruptions at West Mata below a depth of about 2500 m. Nevertheless, we did observe tephra on the recently erupted lava flows, but these deeper deposits were evenly distributed (on and off the new flows) and heavily rippled, suggesting the tephra was transported from areas further upslope and deposited by episodic turbidite-like bottom currents that move fragmental material downslope, as envisioned by Walker et al., under review[4].

The observations also demonstrate that the map-scale morphology of individual eruption deposits is highly dependent on the underlying slope of each site. For example, the "on-rift" eruption sites that are located on relatively steep slopes (sites #1 & 2, and to some extent site #6) are characterized by pillow lava flows that are locally emplaced as "shingled lava plateaus," which form inflated lava flows with slightly domed upper surfaces that are impounded by levees of nearly vertical elongate pillow lavas at their downslope edges, like perched lava-ponds on land. At sites #1 and #2 there is clear evidence that the recent eruptive vents were localized within the headwall scars of previous landslides on the steep margins of the rift zone. We know the landslide at site #2 occurred between December 2010 and November 2011, whereas at site #1 the slide scar had been there since the first bathymetric survey in 1996. There is also ample evidence for landslides occurring during or soon after eruptions where the recent lava flows are cut by scarps exposing truncated pillows in nearly vertical cliffs with local evidence for lava drain-out, showing that parts of the flow interiors were still molten when the landslides occurred. These processes produce ramps of pillow talus and finer clastic debris downslope. In places, late-stage pillow lava flows were also emplaced within the co-eruption landslide chutes, providing additional evidence for the overlap of volcanic construction and mass-wasting processes at the eruption sites on steep slopes.

In contrast, eruption sites on gentler slopes at "off-rift" sites produced a different set of eruption deposits and morphologies. These sites include #4 and #5, which are both located beyond the morphological expression of West Mata's rift zones on flatter terrain off the main edifice (**Figure 2**). At site #4, based on the distinctive morphologies evident in the AUV bathymetry, we interpret that magma first intruded into the sedimented basin as a sill that thickened and uplifted the overlying sediments. Eventually, continued intrusion allowed the magma to reach the surface, probably along faults on the edge of the uplifted sediment, and lava then erupted onto the seafloor and flowed around the domed uplift. This is similar to the scenario envisioned for intrusions/eruptions into sediment on the Escanaba Trough of the Gorda Ridge (NE Pacific) (Denlinger and Holmes, 1994; Morton and Fox, 1994; Zierenberg et al., 2013) and for several locations on the Pescadero and Tamayo transform faults in the Gulf of California (Clague et al., 2018). At site #5, lava flows erupted onto the gently sloping seafloor adjacent to the rift zone and spread out to form low-relief sheet flows. Both sites produced broad lava flows with evidence of inflation and morphologies ranging from pillows to lobate flows to ropy lava, with local tumulus structures that formed due to internal pressure within the molten interior of the sheet-like flows. Co-eruption landslides or auto-brecciation and talus formation were not components of these eruptions on gentler slopes. These two eruption sites are also the deepest documented at West Mata and show that eruptions can take place beyond the obvious morphological limits of the rift zones at the base of the volcano.

Eruption site #3, the pillow ridge on the NE flank of West Mata, is somewhere in between these end-members, in that it has evidence for both constructional pillow lava mounds and local co-eruption mass-wasting on the steeper downslope side of the pillow ridge. On the other hand, it clearly did not form within a previous landslide scar nor on one of West Mata's rift zones, and indeed its location is hard to explain. One possibility is that if it was the last of the three eruptions that occurred between 2012 and 2016, then because the previous two (sites #2 and #4) would have presumably been fed by dikes that intruded along the ENE rift zone, perhaps the compressional stresses across the rift from those intrusions would not have had enough time to relax so that the next dike intrusion was forced to take a different path to the surface. Instead, a dike intruded outward from beneath the summit in a direction close to radial, but outside of the rift zone. Another possibility is that this eruption site was controlled by deeper crustal structure related to the older ridge NE of the volcano. In any case, this must be a relatively rare event based on West Mata's morphology and the lack of other similar examples. It is clear that most eruptions at West Mata occur either at the summit or along the rift zones.

[4]Walker, S. L., Baker, E. T., Lupton, J. E., and Resing, J. A. (under review). Patterns of fine ash dispersal related to volcanic activity at West Mata volcano, NE Lau Basin. *Front. Mar. Sci.*

Common Patterns in Submarine Effusive Volcanism

Despite the differences in tectonic setting and magma composition, the characteristics of the recent eruption deposits at West Mata volcano are notably similar to the results from studies at many other recent submarine eruption sites. In particular, our observations are quite similar to those at other basaltic submarine volcanoes where high-resolution AUV bathymetry and ROV dives allow direct comparisons of map-scale morphology of lava flows and interpretation of their emplacement. Commonalities include the construction of thick hummocky flows of pillow lava with evidence of molten interiors and steep flanks locally modified by co-eruption landslides forming aprons of talus, as well as evidence for inflation of more fluid lava flows on gentler slopes, and intrusion and eruption processes in sedimented basins. Such comparable AUV/ROV datasets include those from the Juan de Fuca and the Gorda spreading ridges and the Alarcon Rise in the NE Pacific (Caress et al., 2012; Chadwick et al., 2013, 2016; Yeo et al., 2013; Zierenberg et al., 2013; Clague et al., 2014, 2017, 2018), the East Pacific Rise (White et al., 2000, 2002; Fornari et al., 2004; Soule et al., 2007; Fundis et al., 2010; Klein et al., 2013; Deschamps et al., 2014), and the Galapagos spreading ridge (Haymon et al., 2008; White et al., 2008; McClinton et al., 2013). The combined results of these high-resolution geological studies show that the effusive eruptive processes we describe here are not unique to West Mata, but are widespread and common to mafic submarine eruptions in diverse tectonic settings, demonstrating their importance on a global scale and a convergence of scientific understanding about submarine effusive volcanism. On the other hand, the significant deposits of pyroclastic tephra at the shallower eruption sites at West Mata are quite unusual, and probably reflect the high volatile content of its boninite parent magma (Resing et al., 2011; Rubin et al., 2018). These tephra deposits and their implications will be the subject of future studies.

This study shows that the combination of high-resolution bathymetry with visual observations of the seafloor and a time-series of repeat mapping surveys can provide insights into the emplacement processes of effusive submarine eruptions. The documentation of multiple eruptive events over a significant depth range illustrates a variety of eruption styles, products, and environments. Observations over an extended period of time reveal the spatial and temporal evolution of volcanic activity, can constrain rates of magma supply, and show how construction and mass wasting events are closely linked.

Recent Eruption History at West Mata

If we consider the history of known eruptions at West Mata since 1996 (**Figure 3**), the most significant change in the character of that activity was the shift from continuous eruptive activity at the summit to episodic eruptions on the rift zones that occurred around early 2011 (although admittedly we know far less about the activity before 2008 than afterward). This change was accompanied or followed closely in time by the collapse of the summit and the formation of Hades crater. It is possible that the site #5 eruption was directly related to the crater collapse, due to magma withdrawal from shallow levels beneath the summit to the deep WSW rift zone, similar to the recent activity at Kilauea volcano, Hawaii (Neal et al., 2019). However, this connection cannot be demonstrated conclusively because the time constraints on the two events are slightly different. Hades crater formed between December 2010 and November 2011, whereas the site #5 eruption occurred between May 2010 and November 2011, but the difference is only because the site #5 eruption was beyond the coverage of the December 2010 multibeam survey (Embley et al., 2014).

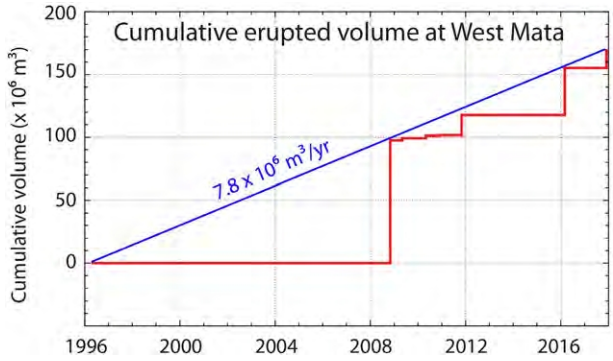

FIGURE 16 | Cumulative erupted volume at West Mata vs. time, based on volumes of depth change between nine repeated ship-based bathymetric surveys listed in **Table 1**. Volumes are from **Table 2** and Embley et al. (2014) and are plotted at the time they were discovered (the second of each pair of surveys). Trend is remarkably linear and implies volume-predictable eruptive behavior in which the volume of the next eruption is predictable from the time since the previous one.

In any case, the transition from continuous to episodic eruptions overlapped in time and it is likely that the onset of activity on the rift zones destabilized the conditions that allowed continuous eruption at the summit. The first three episodic events between 2009 and 2011 were along the WSW rift zone (while activity at the summit was waning), and subsequent events have all been along the ENE rift zone between 2012 and 2018 (after the summit activity had stopped). Over longer periods of time, this distributed volcanism along the rift zones may be the norm at West Mata, intermixed with occasional extended periods of eruptive activity at the summit. Nevertheless, it is remarkable that over the last 22 years the locations of eruptive activity have spanned the entire volcano from the deepest parts of both rift zones, to the summit, to locations in between, and even off the rifts such as on the NE flank. This suggests that when dikes are intruded at West Mata they tend to seek regions within the edifice with relatively low compressive stress, which are likely areas that have not experienced the most recent intrusions and eruptions (Acocella and Neri, 2009). This is similar to the way in which individual dike intrusions were spatially distributed along different parts of the extensional plate boundary during the 1975–1984 Krafla rifting episode in Iceland (Björnsson et al., 1979; Björnsson, 1985; Buck et al., 2006).

The time-series of repeat bathymetry at West Mata allows us to quantify the volume of eruptive products added to the volcano with time. **Figure 16** shows the recent history of cumulative

erupted volume at West Mata, with the volume changes from individual eruptive periods plotted in the year they were discovered (that is, the year of the first subsequent ship-based bathymetric survey), using data from **Table 2** and from Embley et al. (2014). An average linear eruption rate of $\sim 7.8 \times 10^6$ m^3/yr over this time interval fits the cumulative erupted volume time-series remarkably well (**Figure 16**). For comparison, this is about the volume of the 2012–2016 pillow ridge eruption on the NE flank of the volcano (site #3), but most of the other recent eruptions are about twice this volume (**Table 2**), implying an average recurrence interval of about 1–2 years between episodic rift eruptions, which is relatively short. Of course, we have little information about the eruptive activity between 1996 and 2008 – we only know the net volume change between the surveys at the beginning and the end of that period, that most of the volume was added at the summit and on the north flank, and that West Mata was in a state of continuous eruption from the summit near the end of that period. However, it is reasonable to assume that the 1996–2008 erupted volume accumulated over a significant amount of time and that the actual cumulative eruption curve between 1996 and 2008 was probably closer to the longer-term average rate.

If the recent rate of erupted volume at West Mata is approximately linear, it suggests that eruptions are volume-predictable at West Mata, such that the volume of a future eruption can be estimated simply by knowing how much time has elapsed since the previous one. It also suggests that the magma supply is relatively steady over time, which has implications for the underlying magmatic system (Wadge, 1982). The relatively low magma supply rate (for comparison, the magma supply rate to Axial Seamount from 2011 to 2015 was about an order of magnitude higher, Nooner and Chadwick, 2016) and the apparent high frequency of eruptions implies that the magma storage reservoir at West Mata must also be relatively small. In other words, we interpret that a steady rate of magma is being supplied to West Mata's shallow reservoir beneath the summit (at about the long-term eruption rate), but it is only 1–2 years before the pressure within the reservoir exceeds its failure threshold and eruptions occur, which implies the volume of the reservoir is relatively small since it can only accommodate a small increase in volume before failing. Conversely, if the reservoir volume were large, then it would be able to accommodate a small magma supply for longer before eruptions are triggered by high internal pressure. Additional support for this conceptual model comes from the changes in the chemistry of lavas erupted between 2009 and 2011, which are consistent with a small and frequently replenished magma body at West Mata (Rubin et al., 2015, 2018). The apparently low strength of the magma reservoir might be related to the largely clastic character of the volcano. In any case, its recent history implies that West Mata will likely continue to experience frequent eruptions, perhaps every few years, and therefore is an important target for continued re-mapping efforts and perhaps even an ideal candidate for long-term instrumental monitoring. Thus, West Mata continues to be one of the best natural laboratories in the world for the study of active submarine volcanism.

CONCLUSION

The combination of nine repeated ship-based bathymetric surveys, two high-resolution AUV surveys, and the three expeditions that conducted ROV dives provides valuable information about the recent of eruptive history at West Mata submarine volcano since 1996. From this study we make the following conclusions:

(1) The latest two ship-based bathymetric surveys in 2016 and 2017 document four new eruption sites on the ENE rift zone, on the NE flank and at the NE base of the volcano since the previous survey in 2012. AUV and ROV dives in November and December 2017 mapped, sampled, and documented these and other recent eruption sites on the seafloor for the first time.
(2) Early 2011 marked a change in the eruptive behavior of West Mata, from mostly continuous summit activity (1996–2011) to episodic rift eruptions since then (2012–2018).
(3) At the same time, the summit collapsed and the location of subsequent eruptions shifted from the summit and WSW rift zone (1996–2011) to ENE rift zone (2012-present).
(4) Since 2009, there has been an episodic rift eruption every 1–2 years, spanning locations from near the summit to beyond the end of both rift zones at the base of the volcano, a depth range of 1200–3000 mbsl.
(5) These eruptions have had both pyroclastic and effusive components, due to the high volatile content of West Mata's boninite magma. The proportion of tephra decreases with depth, with little or no tephra produced by eruptions below 2500 m. However, downslope tephra transport from shallower parts of the volcano by turbidity currents is common.
(6) The morphology of the recent eruption sites highly depends on the underlying slope, with shingled lava plateaus, landslide scarps, and co-eruption talus more common on steeper slopes, and inflated lava flows with local tumuli but lacking significant fragmental deposits on the gentler slopes at the base of the volcano.
(7) The eruptions at West Mata appear to be volume-predictable with time, suggesting a constant magma supply rate and a relatively small magma storage reservoir that can only accommodate a modest influx of magma between eruptions.
(8) The wide range of recent eruptive sites at West Mata provide well-documented examples of the range of eruption styles and emplacement processes that are common to basaltic submarine volcanoes worldwide.

DATA AVAILABILITY

The data presented in this study are available at the NOAA National Centers for Environmental Information (ship bathymetry), the Rolling Deck to Repository (CTD data

and cruise reports), the IEDA Marine Geoscience Data System (AUV *Sentry* and ROV *SuBastian* data), and ROV video is available on the Schmidt Ocean Institute YouTube channel.

AUTHOR CONTRIBUTIONS

WC wrote the manuscript, made the figures and tables, and was co-chief scientist on the FK171110 expedition. KR was chief scientist on that expedition and co-directed the ROV dives described here. SM processed and analyzed ship-based and AUV-based multibeam sonar bathymetric data. SM and AB assisted with GIS data management, volume calculations, and figure preparation. TK was chief scientist on the FK160320 expedition and collected the 2016 multibeam bathymetric survey. RE helped to interpret the new results in the context of previous observations at West Mata.

FUNDING

We gratefully acknowledge the funding of the NOAA Ocean Exploration and Research (OER) Program and NOAA's Pacific Marine Environmental Laboratory (PMEL) for support of the science at sea and on shore. This research was supported by the PMEL Earth-Ocean Interactions Program and the Cooperative Institute for Marine Resources Studies (CIMRS) under NOAA Cooperative Agreement NA11OAR4320091 and NA15OAR4320063. Ship time on *R/V Falkor* and use of AUV *Sentry* on expedition FK171110 were supported by the Schmidt Ocean Institute.

ACKNOWLEDGMENTS

We thank the Schmidt Ocean Institute for supporting expeditions FK160320 and FK171110 on *R/V Falkor*, as well as the ship's crews and the teams that operated AUV *Sentry* and ROV *SuBastian*, especially expedition leaders Sean Kelley (AUV *Sentry*) and Russell Coffield (ROV *SuBastian*). We also thank the science parties of ROV expeditions TN234, RR1211, and FK171110, who contributed to their success. In addition, we thank Dave Clague, Dave Caress, and Jenny Paduan at MBARI for making the high-resolution data available from the AUV *D. Allan B.* dives at West Mata in 2009 and for helpful comments on an early draft of the manuscript. The text was also improved by the helpful comments from the two reviewers. PMEL contribution number 4927. SOEST contribution number 10724.

REFERENCES

Acocella, V., and Neri, M. (2009). Dike propagation in volcanic edifices: overview and possible developments. *Tectonophysics* 471, 67–77. doi: 10.1016/j.tecto.2008.10.002

Allen, R. W., Berry, C., Henstock, T. J., Collier, J. S., Dondin, F. J.-Y., Rietbrock, A., et al. (2018). 30 years in the life of an active submarine volcano: a time - lapse bathymetry study of the Kick 'em Jenny volcano, Lesser Antilles. *Geochem. Geophys. Geosyst.* 19, 715–731. doi: 10.1002/2017GC007270

Appelgate, B., and Embley, R. W. (1992). Submarine tumuli and inflated tube-fed lava flows on Axial Volcano, Juan de Fuca Ridge. *Bull. Volcanol.* 54, 447–458. doi: 10.1007/bf00301391

Baker, E. T., Walker, S. L., Massoth, G. J., and Resing, J. A. (2019). The NE Lau Basin: widespread and abundant hydrothermal venting in the back-arc region behind a superfast subduction zone. *Front. Mar. Sci.* 6:382. doi: 10.3389/fmars.2019.00382

Baumberger, T., Lilley, M. D., Resing, J. A., Lupton, J. E., Baker, E. T., Butterfield, D. A., et al. (2014). Understanding a submarine eruption through time series hydrothermal plume sampling of dissolved and particulate constituents: West Mata, 2008–2012. *Geochem. Geophys. Geosyst.* 15, 4631–4650. doi: 10.1002/2014GC005460

Bevis, M., Taylor, F. W., Schutz, B. E., Recy, J., Isacks, B. L., Helu, S., et al. (1995). Geodetic observations of very rapid convergence and back-arc extension at the Tonga arc. *Nature* 374, 249–251. doi: 10.1038/374249a0

Björnsson, A. (1985). Dynamics of crustal rifting in NE Iceland. *J. Geophys. Res.* 90, 10151–10162.

Björnsson, A., Johnsen, G., Sigurdsson, S., Thorbergsson, G., and Tryggvason, E. (1979). Rifting of the plate boundary in north Iceland, 1975-1978. *J. Geophys. Res.* 84, 3029–3038.

Bohnenstiehl, D. R., Dziak, R. P., Matsumoto, H., and Conder, J. A. (2014). Acoustic response of submarine volcanoes in the Tofua Arc and northern Lau Basin to two great earthquakes. *Geophys. J. Int.* 196, 1657–1675. doi: 10.1093/gji/ggt472

Buck, W. R., Einarsson, P., and Brandsdottir, B. (2006). Tectonic stress and magma chamber size as controls on dike propagation: constraints from the 1975–1984 Krafla rifting episode. *J. Geophys. Res.* 111:B12404. doi: 10.1029/2005JB003879

Caplan-Auerbach, J., Dziak, R. P., Bohnenstiehl, D. R., Chadwick, W. W. Jr., and Lau, T.-K. A. (2014). Hydroacoustic investigation of submarine landslides at West Mata volcano, Lau Basin. *Geophys. Res. Lett.* 41, 5927–5934. doi: 10.1002/2014GL060964

Caress, D. W., and Chayes, D. N. (2016). *MB-System: Mapping the Seafloor*. Available at: http://www.mbari.org/data/mbsystem/[Online] and software version is v5.5 (accessed September 15, 2016).

Caress, D. W., Clague, D. A., Paduan, J. B., Martin, J., Dreyer, B., Chadwick, W. W. Jr., et al. (2012). Repeat bathymetric surveys at 1-metre resolution of lava flows erupted at Axial Seamount in April 2011. *Nat. Geosci.* 5, 483–488. doi: 10.1038/NGEO1496

Chadwick, W. W. Jr., Cashman, K. V., Embley, R. W., Matsumoto, H., Dziak, R. P., de Ronde, C. E. J., et al. (2008). Direct video and hydrophone observations of submarine explosive eruptions at NW Rota-1 volcano, Mariana arc. *J. Geophys. Res.* 113:B08S10. doi: 10.1029/2007JB005215

Chadwick, W. W. Jr., Clague, D. A., Embley, R. W., Perfit, M. R., Butterfield, D. A., Caress, D. W., et al. (2013). The 1998 eruption of Axial Seamount: new insights on submarine lava flow emplacement from high-resolution mapping. *Geochem. Geophys. Geosyst.* 14, 3939–3968. doi: 10.1002/ggge20202

Chadwick, W. W. Jr., Dziak, R. P., Haxel, J. H., Embley, R. W., and Matsumoto, H. (2012). Submarine landslide triggered by volcanic eruption recorded by in-situ hydrophone. *Geology* 40, 51–54. doi: 10.1130/G32495.1

Chadwick, W. W. Jr., Paduan, B. P., Clague, D. A., Dreyer, B. M., Merle, S. G., Bobbitt, A. M., et al. (2016). Voluminous eruption from a zoned magma body after an increase in supply rate at Axial Seamount. *Geophys. Res. Lett.* 43, 12063–12070. doi: 10.1002/2016GL071327

Clague, D. A. (2015). *Processed Near-Bottom Multibeam Sonar Data (version 2) from the Lau Back-Arc Basin Acquired with AUV D. Allan B. During the Thomas G. Thompson Expedition TN234 (2009)*. Palisades, NY: Interdisciplinary Earth Data Alliance. doi: 10.1594/IEDA/316787

Clague, D. A., Caress, D. W., Dreyer, B. M., Lundsten, L. J., Paduan, J. B., Portner, R. A., et al. (2018). Geology of the Alarcon Rise, southern Gulf of California. *Geochem. Geophys. Geosyst.* 19, 807–837. doi: 10.1002/2017GC007348

Clague, D. A., Dreyer, B. M., Paduan, J. B., Martin, J. F., Caress, D. W., Gill, J. B., et al. (2014). Eruptive and tectonic history of the Endeavour Segment, Juan de

Fuca Ridge, based on AUV mapping data and lava flow ages. *Geochem. Geophys. Geosyst.* 15, 3364–3391. doi: 10.1002/2014GC005415

Clague, D. A., Paduan, J. B., Caress, D. W., Chadwick, W. W. Jr., Saout, M. L., Dreyer, B., et al. (2017). High-resolution AUV mapping and targeted ROV observations of three historical lava flows at Axial Seamount. *Oceanography* 30, 82–99. doi: 10.5670/oceanog.2017.426

Clague, D. A., Paduan, J. B., Caress, D. W., Thomas, H., Chadwick, W. W. Jr., and Merle, S. G. (2011). Volcanic morphology of West Mata Volcano, NE Lau Basin, based on high-resolution bathymetry and depth changes. *Geochem. Geophys. Geosyst.* 12:QOAF03. doi: 10.1029/2011GC003791

Crisp, J. A. (1984). Rates of magma emplacement and volcanic output. *J. Volcanol. Geotherm. Res.* 20, 177–211. doi: 10.1016/0377-0273(84)90039-8

Deardorff, N. D., Cashman, K. V., and Chadwick, W. W. Jr. (2011). Observations of eruptive plumes and pyroclastic deposits from submarine explosive eruptions at NW Rota-1. Mariana Arc. *J. Volcanol. Geothermal Res.* 202, 47–59. doi: 10.1016/j.jvolgeores.2011.01.003

Denlinger, R. P., and Holmes, M. L. (1994). "A thermal and mechanical model for sediment hills and associated sulfide deposits along escanaba trough," in *Geologic, Hydrothermal, and Biologic Studies at Escanaba Trough, Gorda Ridge, Offshore Northern California*, eds J. L. Morton, R. A. Zierenberg, and C. A. Reiss (Virginia, VA: U.S. Geological Survey), 65–75.

Deschamps, A., Grigné, C., Le Saout, M., Soule, S. A., Allemand, P., Van Vliet Lanoe, B., et al. (2014). Morphology and dynamics of inflated subaqueous basaltic lava flows. *Geochem. Geophys. Geosyst.* 15, 2128–2150. doi: 10.1002/2014GC005274

Dziak, R. P., Bohnenstiehl, D. R., Baker, E. T., Matsumoto, H., Caplan-Auerbach, J., Embley, R. W., et al. (2015). Long-term explosive degassing and debris flow activity at West Mata submarine volcano. *Geophys. Res. Lett.* 42, 1480–1487. doi: 10.1002/2014GL062603

Embley, R. W., Chadwick, W. W. Jr., Baker, E. T., Butterfield, D. A., Resing, J. A., De Ronde, C. E. J., et al. (2006). Long-term eruptive activity at a submarine arc volcano. *Nature* 441, 494–497. doi: 10.1038/nature04762

Embley, R. W., Merle, S. G., Baker, E. T., Rubin, K. H., Lupton, J. E., Resing, J. A., et al. (2014). Eruptive modes and hiatus of volcanism at West Mata seamount, NE Lau Basin: 1996-2012. *Geochem. Geophys. Geosyst.* 15, 4093–4115. doi: 10.1002/2014GC005387

Embley, R. W., and Rubin, K. H. (2018). Extensive young silicic volcanism produces large deep submarine lava flows in the NE Lau Basin. *Bull. Volcanol.* 80:36.

Fornari, D. J., Tivey, M. A., Schouten, H., Perfit, M., Yoerger, D., Bradley, A., et al. (2004). "Submarine lava flow emplacement at the East Pacific Rise 9°50'N: Implications for uppermost ocean crust stratigraphy and hydrothermal fluid circulation," in *Mid-Ocean Ridges: Hydrothermal Interactions Between the Lithosphere and Oceans*, eds C. R. German, J. Lin, and L. M. Parson (Washington, DC: American Geophysical Union), 187–217. doi: 10.1029/148gm08

Fundis, A. T., Soule, S. A., Fornari, D. J., and Perfit, M. R. (2010). Paving the seafloor: volcanic emplacement processes during the 2005-2006 eruptions at the fast spreading East Pacific Rise, 9°50'N. *Geochem. Geophys. Geosyst.* 11:Q08024. doi: 10.1029/2010GC003058

Haymon, R. M., White, S. M., Baker, E. T., Anderson, P. G., Macdonald, K. C., and Resing, J. A. (2008). High-resolution surveys along the hot spot – affected Galapagos Spreading Center: 3. Black smoker discoveries and the implications for geological controls on hydrothermal activity. *Geochem. Geophys. Geosyst.* 9:Q12006.

Klein, E. M., White, S. M., Nunnery, J. A., Mason-Stack, J. L., Wanless, V. D., Perfit, M. R., et al. (2013). Seafloor photo-geology and sonar terrain modeling at the 9°N overlapping spreading center, East Pacific Rise. *Geochem. Geophys. Geosyst.* 14, 5146–5170. doi: 10.1002/2013GC004858

McClinton, T., White, S. M., Colman, A., and Sinton, J. M. (2013). Reconstructing lava flow emplacement processes at the hotspot-affected Galapagos Spreading Center, 95°W and 92°W. *Geochem. Geophys. Geosyst.* 14, 2731–2756. doi: 10.1002/ggge.20157

Merle, S., Chadwick, W., and Rubin, K. (2018a). *Processed Gridded Near-Bottom AUV Sentry Bathymetric Sonar Data (NetCDF:GMT format) from the NE Lau Basin Acquired During Falkor Expedition FK171110 (2017).* Palisades, NY: Interdisciplinary Earth Data Alliance. doi: 10.1594/IEDA/324499

Merle, S. M., Chadwick, W. W. Jr., and Rubin, K. H. (2018b). *Processed Gridded Bathymetry Data from the Tonga Volcanic Arc acquired during R/V Falkor Expedition FK171110 (2017).* Palisades, NY: Interdisciplinary Earth Data Alliance. doi: 10.1594/IEDA/324447

Morton, J. L., and Fox, C. G. (1994). "Structural setting and interaction of volcanism and sedimentation at Escanaba Trough: geophysical results," in *Geologic, Hydrothermal, and Biologic Studies at Escanaba Trough, Gorda Ridge, Offshore Northern California*, eds J. L. Morton, R. A. Zierenberg, and C. A. Reiss (Virginia, VA: United States Geological Survey), 21–44.

Neal, C. A., Brantley, S. R., Antolik, L., Babb, J. L., Burgess, M., Calles, K., et al. (2019). The 2018 rift eruption and summit collapse of Kilauea Volcano. *Science* 363, 367–374. doi: 10.1126/science.aav7046

Nooner, S. L., and Chadwick, W. W. Jr. (2016). Inflation-predictable behavior and co-eruption deformation at Axial Seamount. *Science* 354, 1399–1403. doi: 10.1126/science.aah4666

Resing, J. A., Rubin, K. H., Embley, R. W., Lupton, J. E., Baker, E. T., Dziak, R. P., et al. (2011). Active submarine eruption of boninite in the northeastern Lau Basin. *Nat. Geosci.* 4, 799–806. doi: 10.1038/NGEO1275

Rubin, K. H., Chadwick, W. W. Jr., Embley, R. W., Merle, S. G., Shank, T. M., Cho, W., et al. (2018). "Exploration of the Mata Submarine Volcano Group Reveals Volcano-Tectonic-Hydrothermal Links," in *Abstract V14A-08 presented at 2018 Fall Meeting* (Washington, DC: AGU).

Rubin, K. H., Michael, P., Jenner, F., Clague, D., Glancy, S., Hellebrand, E., et al. (2015). "Composition within and between Tonga arc/Lau Basin backarc eruptions reveal wide variety of parent melts linked to eruption styles," in *Proceedings of the Goldschmidt Conference Abstracts*, Prague.

Rubin, K. H., Soule, S. A., Chadwick, W. W. Jr., Fornari, D. J., Clague, D. A., Embley, R. W., et al. (2012). Volcanic eruptions in the deep sea. *Oceanography* 25, 142–157. doi: 10.5670/oceanog.2012.12

Schnur, S. R., Chadwick, W. W. Jr., Embley, R. W., Ferrini, V. L., De Ronde, C. E. J., Cashman, K. V., et al. (2017). A decade of volcanic construction and destruction at the summit of NW Rota-1 seamount: 2004–2014. *J. Geophys. Res.* 122, 1558–1584. doi: 10.1002/2016JB013742

Soule, S. A., Fornari, D. J., Perfit, M. R., and Rubin, K. H. (2007). New insights into mid-ocean ridge volcanic processes from the 2005–2006 eruption of the East Pacific Rise, 9°46'N–9°56'N. *Geology* 35, 1079–1082.

Staudigel, H., Hart, S. R., Pile, A., Bailey, B. E., Baker, E. T., Brooke, S., et al. (2006). Vailulu'u Seamount, Samoa: Life and death on an active submarine volcano. *Proc. Natl. Acad. Sci. U.S.A.* 103, 6448–6453. doi: 10.1073/pnas.0600830103

Wadge, G. (1982). Steady state volcanism: evidence from eruption histories of polygenetic volcanoes. *J. Geophys. Res.* 87, 4035–4049.

Walker, G. P. L. (1991). Structure, and origin by injection of lava under surface crust, of tumuli, "lava rises", "lava-rise pits", and "lava-inflation clefts" in Hawaii. *Bull. Volcanol.* 53, 546–558. doi: 10.1007/bf00298155

Watts, A. B., Peirce, C., Grevemeyer, I., Pauletto, M., Stratford, W. R., Bassett, D., et al. (2012). Rapid rates of growth and collapse of Monowai submarine volcano in the Kermadec Arc. *Nat. Geosci.* 5, 510–515. doi: 10.1038/ngeo1473 doi: 10.1038/ngeo1473

White, S. M., Macdonald, K. C., and Haymon, R. M. (2000). Basaltic lava domes, lava lakes, and volcanic segmentation on the southern East Pacific Rise. *J. Geophys. Res.* 103, 25519–25536.

White, S. M., Macdonald, K. C., and Sinton, J. M. (2002). Volcanic mound fields on the East Pacific Rise, 16°-19°S: low effusion rate eruptions at overlapping spreading centers for the past 1 Myr. *J. Geophys. Res.* 107:2240.

White, S. M., Meyer, J. D., Haymon, R. M., Macdonald, K. C., Baker, E. T., and Resing, J. A. (2008). High-resolution surveys along the hot spot – affected Galapagos Spreading Center: 2. Influence of magma supply on volcanic morphology. *Geochem. Geophys. Geosyst.* 9:Q09004.

Wilcock, W. S. D., Dziak, R. P., Tolstoy, M., Chadwick, W. W. Jr., Nooner, S. L., Bohnenstiehl, D. R., et al. (2018). The recent volcanic history of Axial Seamount: geophysical insights into past eruption dynamics with an eye toward

enhanced observations of future eruptions. *Oceanography* 31, 114–123. doi: 10.5670/oceanog.2018.117

Yeo, I. A., Clague, D. A., Martin, J. F., Paduan, J. B., and Caress, D. W. (2013). Preeruptive flow focussing in dikes feeding historical pillow ridges on the Juan de Fuca and Gorda Ridges. *Geochem. Geophys. Geosyst.* 14, 3586–3599. doi: 10.1002/ggge.20210

Zellmer, K. E., and Taylor, B. (2001). A three-plate kinematic model for Lau Basin opening. *Geochem. Geophys. Geosyst.* 2, 1–26. doi: 10.1029/2000GC000106

Zierenberg, R. A., Clague, D. A., Paduan, J. B., and Caress, D. W. (2013). New maps focus 30-odd years of investigation of the Escanaba Trough spreading center. *Geol. Soc. Am. Abstr. Programs* 47:381.

Conflict of Interest Statement: The authors declare that the research was conducted in the absence of any commercial or financial relationships that could be construed as a potential conflict of interest.